ChemPubSoc Europe

DOI: 10.1002/chem.201305084

CHEMISTRY
A European Journal
Full Paper

Metal–Arylamides/Aylimides

# Ruthenium Porphyrins with Axial π-Conjugated Arylamide and Arylimide Ligands

Siu-Man Law,[a] Daqing Chen,[a] Sharon Lai-Fung Chan,[c] Xiangguo Guan,[a] Wai-Man Tsui,[a] Jie-Sheng Huang,[a] Nianyong Zhu,[a] and Chi-Ming Che*[a, b]

**Abstract:** A series of ruthenium porphyrins [$Ru^{IV}$(por)$(NHY)_2$] and [$Ru^{VI}$(por)$(NY)_2$] bearing axially coordinated π-conjugated arylamide and arylimide ligands, respectively, have been synthesized. The crystal structures of [$Ru^{IV}$(tmp)$(NHY)_2$] (tmp = 5,10,15,20-tetramesitylporphyrinato(2−)) with Y = 4′-methoxy-biphenyl-4-yl (**Ar**–**Ar**-*p*-OMe), 4′-chloro-biphenyl-4-yl (**Ar**–**Ar**-*p*-Cl), and 9,9-dibutyl-fluoren-2-yl (**Ar**^**Ar**) show axial Ru–N(arylamide) distances of 1.978(4), 1.971(6), and 1.985(13) Å, respectively. [$Ru^{IV}$(tmp)(NH{**Ar**^**Ar**})$_2$] is an example of metalloporphyrins that bind an arylamide ligand featuring a co-planar biphenyl unit. The [$Ru^{IV}$(por)$(NHY)_2$] complexes show a quasi-reversible reduction couple or irreversible reduction wave attributed to $Ru^{IV} \rightarrow Ru^{III}$ with $E_{pc}$ from −1.06 to −1.40 V versus $Cp_2Fe^{+/0}$ and an irreversible oxidation wave with $E_{pa}$ from −0.04 to 0.19 V versus $Cp_2Fe^{+/0}$. Reaction of the [$Ru^{IV}$(por)$(NHY)_2$] with bromine afforded [$Ru^{IV}$(por)(NHY)Br]. $PhI(OAc)_2$ oxidation of the [$Ru^{IV}$(por)$(NHY)_2$] gave [$Ru^{VI}$(por)$(NY)_2$]; the latter can be prepared from reaction of [$Ru^{II}$(por)(CO)] with aryl azides $N_3Y$. The crystal structure of [$Ru^{VI}$(tmp)(N{**Ar**–**Ar**-*p*-OMe})$_2$] features Ru–N(arylimide) distances of 1.824(5) and 1.829(5) Å. Alkene aziridination and C–H amination catalyzed by "[$Ru^{II}$(tmp)(CO)] + π-conjugated aryl azides", or mediated by [$Ru^{VI}$(por)$(NY)_2$] with Y = biphenyl-4-yl (**Ar**–**Ar**) and **Ar**–**Ar**-*p*-Cl, gave aziridines and amines in moderate yields. The electronic structure of [$Ru^{VI}$(por)$(NY)_2$] was examined by DFT calculations.

## Introduction

Studies on metal-to-ligand π-back-bonding interactions in low-valent metal complexes containing π-acid ligands prevail in inorganic and organometallic chemistry.[1] Of equal importance are metal-ligand π-bonding interactions that are prevelant in high-valent metal complexes.[2] In our endeavor to exploit metal–nitrogen π-bonding interaction as a means for electronic communication between redox active metal ions and remote functional groups over a long distance, we are interested in metalloporphyrins[3] axially coordinated with π-conjugated arylamide and arylimide ligands that possess mutually conjugated phenyl groups. These types of π-conjugated arylamide/arylimide ligands coordinated to transition metals are sparsely seen in the literature; we noted a few such examples, which belong to metal–mono(amide) or *cis*-metal–bis(amide) complexes[4] or metal–mono(imide) complexes (**A** and **B** in Figure 1).[5] Despite the reports of a number of metalloporphyrin arylamide[6–8] and arylimide[5b,8–13] complexes, we are aware of one such complex, [$V^{IV}$(ttp)(N{**Ar**–**Ar**})] (**Ar**–**Ar** = biphenyl-4-yl),[3,5b] that bears mutually conjugated phenyl groups in the

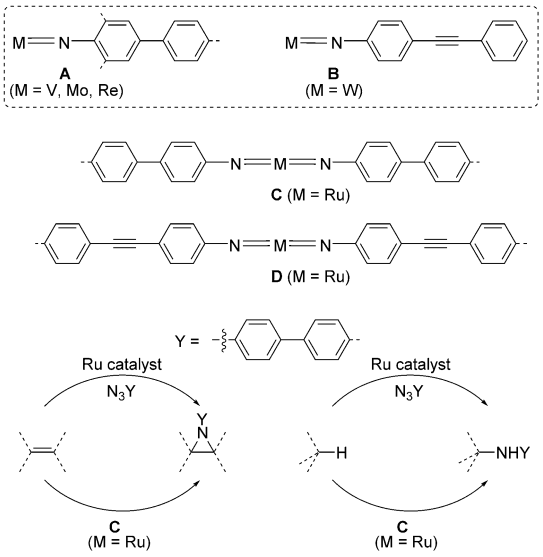


**Figure 1.** Types of metal complexes with π-conjugated imides, and the corresponding catalytic and stoichiometric nitrogen group transfer/insertion reactions, reported in this work. Inset: literature-reported metal complexes with π-conjugated imides.

[a] *S.-M. Law, Dr. D. Chen, Dr. X. Guan, Dr. W.-M. Tsui, Dr. J.-S. Huang, Dr. N. Zhu, Prof. Dr. C.-M. Che*
*Department of Chemistry and State Key Laboratory of Synthetic Chemistry*
*The University of Hong Kong, Pokfulam Road, Hong Kong (P. R. China)*
*E-mail: cmche@hku.hk*

[b] *Prof. Dr. C.-M. Che*
*HKU Shenzhen Institute of Research and Innovation*
*Shenzhen 518053 (P. R. China)*

[c] *Dr. S. L.-F. Chan*
*Department of Applied Biology and Chemical Technology*
*The Hong Kong Polytechnic University*
*Hung Hom, Kowloon, Hong Kong (P. R. China)*

*Supporting information for this article is available on the WWW under http://dx.doi.org/10.1002/chem.201305084.*

axial ligand. Cenini, Gallo, and co-workers reported the synthesis of [Ru$^{VI}$(tpp)(N{Ar-3,5-$CF_3$}$_2$)$_2$] (Ar-3,5-$CF_3$ = 3,5-di(trifluoromethyl)phenyl),[3,8] which has been characterized by X-ray crystal structure analysis. It should be noted that there are examples of reactive metal–arylimide non-porphyrin complexes such as the ones reported by Hillhouse,[14a,b] Betley,[14c] and co-workers.

Metalloporphyrin complexes of π-conjugated arylimides/arylnitrenes are also of importance in C–N bond formation via metal-catalyzed nitrogen group transfer/insertion reactions, like sulfonylimide and simple arylimide complexes of ruthenium porphyrins [Ru$^{VI}$(por)($NSO_2Y$)$_2$][15] and [Ru$^{VI}$(tpp)(N{Ar-3,5-$CF_3$}$_2$)$_2$][3,8] both of which are reactive toward C–H amination of hydrocarbons. Examples of π-conjugated arylnitrenes generated by photolysis of the corresponding aryl azides have been documented,[16,17] and the photolytically generated biphenyl-2-yl nitrene undergoes intramolecular C–H insertion reaction.[18] There are several reports on metal-catalyzed C–N bond forming reactions[19–21] which possibly involve reactive metal–mono(imide/nitrene) intermediates including Rh or Fe complexes of biphenyl-4-yl imides/nitrenes[19,20] and Rh or Ru complexes of biphenyl-2-yl imides/nitrenes.[21] But the transfer/insertion of π-conjugated arylimides/arylnitrenes from their well-characterized complexes of transition metals to hydrocarbons has been little (if at all) explored.

Herein we report the syntheses, characterization, and reactivity of a series of *trans*-bis(π-conjugated arylamide) and *trans*-bis(π-conjugated arylimide) complexes (**C** and **D** in Figure 1) of ruthenium porphyrins: [Ru$^{IV}$(por)($NHY$)$_2$] (Scheme 1) and [Ru$^{VI}$(por)($NY$)$_2$] (Scheme 2), respectively. Nitrogen group transfer/insertion reactions of these [Ru$^{VI}$(por)($NY$)$_2$] complexes with alkenes/C–H bonds have been observed to give aziridination/amination products; the corresponding catalytic intermolecular aziridination/amination of alkenes/C–H bonds has been achieved using a "[Ru$^{II}$(por)(CO)] + π-conjugated aryl azide" protocol (Figure 1). Also reported herein are the electrochemical studies on [Ru$^{IV}$(por)($NHY$)$_2$] and the reactions of [Ru$^{IV}$(por)($NHY$)$_2$] with $Br_2$ and $PhI(OAc)_2$ to give [Ru$^{IV}$(por)(NHY)Br] and [Ru$^{VI}$(por)($NY$)$_2$], respectively, together with the studies of the electronic structure of [Ru$^{VI}$(por)($NY$)$_2$] by density functional theory (DFT) calculations.

## Results and Discussion

### Synthesis

The ruthenium porphyrin complexes synthesized in this work and the abbreviations for various π-conjugated aryl groups (in bold face) including **Ar^Ar** that bears a co-planar biphenyl unit, along with those for simple aryl groups (in plain face), are listed in Table 1. The abbreviations for the porphyrin ligands are included in ref. [3] (see also the inset of Scheme 1).

**Bis(π-conjugated arylamide) complexes**: Treatment of the dioxoruthenium(VI) porphyrin [Ru$^{VI}$(tmp)$O_2$] with excess amounts of π-conjugated arylamines $NH_2Y$ including $NH_2$(**Ar**–**Ar**), $NH_2$(**Ar**–**Ar**-*p*-OMe), $NH_2$(**Ar**–**Ar**-*p*-Cl), $NH_2$(**Ar^Ar**), $NH_2$(**Ar**–**Ar**–**Ar**), $NH_2$(**Ar**–**C**≡**C**–**Ar**), and $NH_2$(**Ar**–**C**≡**C**–**Ar**–**C**≡**C**–**Ar**), in aerobic ethanol or dichloromethane for 8 h afforded the corresponding [Ru$^{IV}$(tmp)($NHY$)$_2$] (**1**, Scheme 1 and entries 1–7 in Table 1) in 54–73% yields. Complexes [Ru$^{IV}$(por)(NH{**Ar**–**Ar**})$_2$] (por = ttp, 3,4,5-OMe-tpp) and [Ru$^{IV}$(por)(NH{**Ar^Ar**})$_2$] (por = ttp, 4-OMe-tpp, 4-Cl-tpp) were prepared in 52–76% yields from similar reactions (entries 8–12, Table 1). We also treated [Ru$^{VI}$(ttp)$O_2$] with $NH_2$(**Ar**–**C**≡**C**–**Ar**) and $NH_2$(**Ar**–**C**≡**C**–**Ar**–**C**≡**C**–**Ar**); these reactions did not give the corresponding [Ru$^{IV}$(ttp)($NHY$)$_2$]. When [Ru$^{VI}$($F_{20}$-tpp)$O_2$] was treated with $NH_2${**Ar^Ar**}, and also $NH_2$(Ar-*p*-X) (X = Cl, NHPh), under similar reaction conditions, bis(arylamine)ruthenium(II) porphyrins [Ru$^{II}$($F_{20}$-tpp)($NH_2Y$)$_2$] (**2**, Scheme 1 and entries 16–18 in Table 1) were obtained in 20–50% yields. In contrast, [Ru$^{II}$(por)($NH_2${**Ar^Ar**})$_2$] (por = tmp, ttp, 4-OMe-tpp, 4-Cl-tpp, 3,4,5-OMe-tpp) were not detected in the final reaction mixtures of the corresponding [Ru$^{VI}$(por)$O_2$] with $NH_2$(**Ar^Ar**) as revealed by UV/Vis and $^1$H NMR spectroscopy. Upon stirring a solution of [Ru$^{II}$($F_{20}$-tpp)($NH_2${**Ar^Ar**})$_2$] in aerobic dichloromethane for 5 days, [Ru$^{IV}$($F_{20}$-tpp)(NH{**Ar^Ar**})$_2$] was obtained in 95% yield.

We previously prepared [Ru$^{IV}$(por)($NPh_2$)$_2$] (por = 3,4,5-OMe-tpp; 3,5-Cl-tpp)[6b,d] and [Ru$^{IV}$(por)(NH{Ar-*p*-X})$_2$] (por = ttp, 4-Cl-tpp; X = Cl, $NO_2$)[6d] from the reactions of [Ru$^{VI}$(por)$O_2$] with $NHPh_2$ and $NH_2$(Ar-*p*-X), respectively. Similarly, [Ru$^{IV}$(por)(NH{Ar-*p*-Cl})$_2$] (por = tmp, 4-OMe-tpp) were prepared in 78–88% yields in this work (entries 14 and 15, Table 1). The reactions of [Ru$^{VI}$(por)$O_2$] with alkylamines[6d,22,23] and amino esters[24] were reported to afford bis(amine)ruthenium(II) porphyrins. Other related reactivity of [Ru$^{VI}$(por)$O_2$] include the reaction with benzophenone imine to give [Ru$^{IV}$(por)(N=$CPh_2$)$_2$][22b] or [Ru$^{II}$(por)(NH=$CPh_2$)$_2$],[25] and the reaction with 1,1-diphenylhydrazine to give [Ru$^{IV}$(por)($NHNPh_2$)$_2$].[26]

The formation of [Ru$^{IV}$(por)($NHY$)$_2$] from reaction of [Ru$^{VI}$(por)$O_2$] with excess amounts of $NH_2Y$ in aerobic solutions is likely to proceed through intermediates [Ru$^{II}$(por)($NH_2Y$)$_2$]; the latter underwent oxidative deprotonation by air to give the arylamide complexes.[6d] Indeed, in the course of the synthesis of [Ru$^{IV}$(3,4,5-OMe-tpp)(NH{**Ar**–**Ar**})$_2$], the UV/Vis absorption spectrum of the reaction mixture first showed Soret and β bands at approximately 418 and 505 nm, respectively (reaction time: ~30 min), which are characteristic of bis(amine)ruthenium(II) porphyrins.[6d] Further evidence is the above-mentioned isolation of [Ru$^{II}$($F_{20}$-tpp)($NH_2Y$)$_2$], instead of [Ru$^{IV}$($F_{20}$-tpp)($NHY$)$_2$], for the reactions with $NH_2$(**Ar^Ar**) and $NH_2$(Ar-*p*-X) (X = Cl, NHPh) at a reaction time of 8 h, coupled with the nearly quantitative conversion of [Ru$^{II}$($F_{20}$-tpp)($NH_2${**Ar^Ar**})$_2$] to [Ru$^{IV}$($F_{20}$-tpp)(NH{**Ar^Ar**})$_2$] by autoxidation for 5 days. The high stability of [Ru$^{II}$($F_{20}$-tpp)($NH_2Y$)$_2$] can be attributed to the relatively electron-deficient $F_{20}$-tpp ligand, which renders the Ru$^{II}$ complexes less prone to undergo oxidative deprotonation. For comparison, [Ru$^{II}$(por)($NH_2${Ar-*p*-Cl})$_2$] (por = ttp, 4-Cl-tpp) rapidly undergo autooxidation to [Ru$^{IV}$(por)(NH{Ar-*p*-Cl})$_2$] in aerobic solutions within 0.5–1.5 h.[6d]

The fate of arylamines upon oxidation by [Ru$^{VI}$(por)$O_2$] was examined using $NH_2$(**Ar**–**Ar**) and $NH_2$(Ar-*p*-Cl) as examples, which were found to be oxidized to Y–N=N–Y (Y = **Ar**–**Ar**, Ar-*p*-Cl) in 55 and 48% yields, respectively. Such Y–N=N–Y compounds were previously formed through, for example, amine

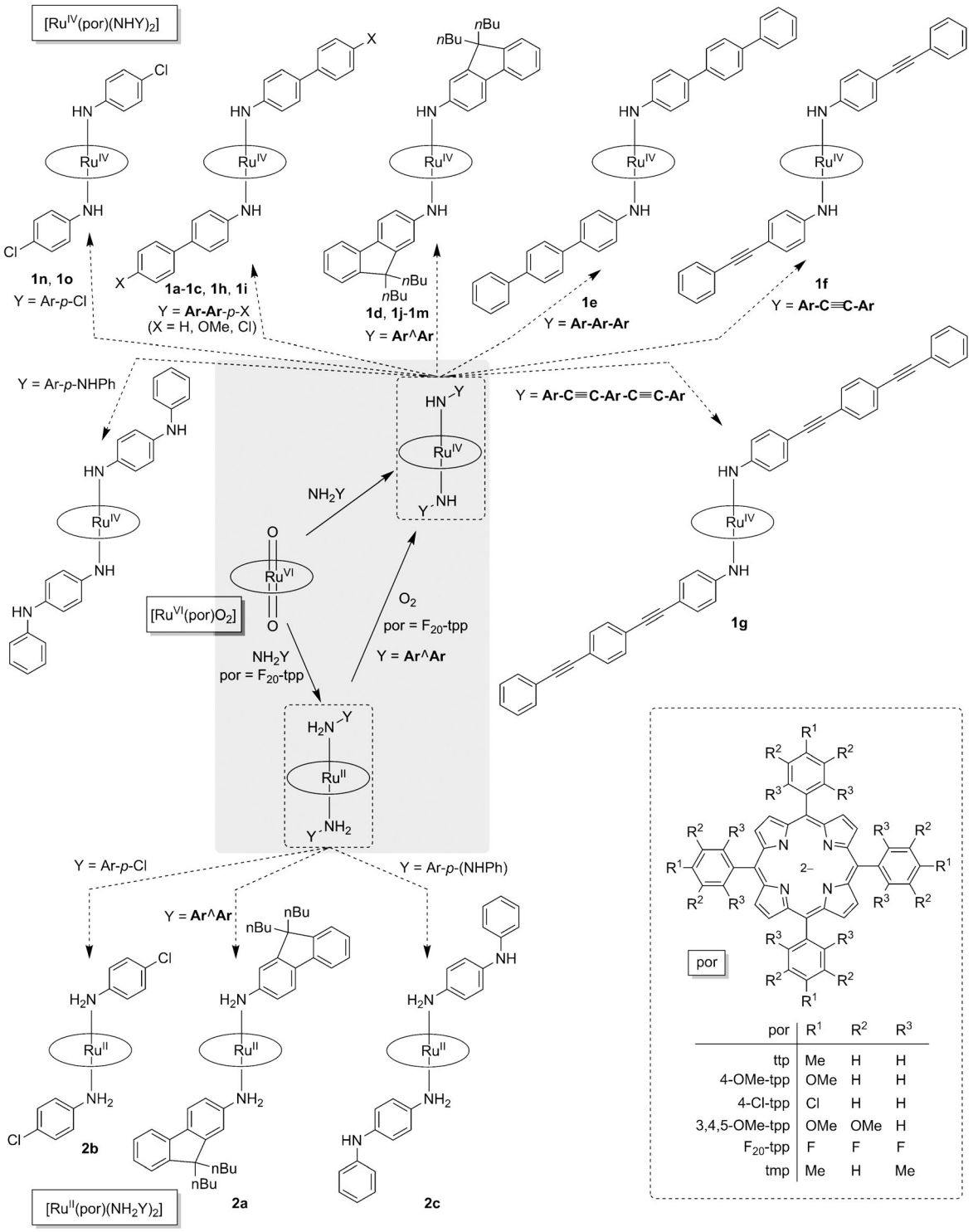


**Scheme 1.** Syntheses of $[Ru^{IV}(por)(NHY)_2]$ (**1**) from reaction of $[Ru^{VI}(por)O_2]$ with $NH_2Y$ or from oxidative deprotonation of $[Ru^{II}(por)(NH_2Y)_2]$ (**2**). Inset: porphyrinato(2−) ligands employed in this work.

oxidation with $KMnO_4$ catalyzed by $FeSO_4{\cdot}7H_2O$[27] or $CuSO_4$ and $Al_2O_3$,[28] by treating the amine with HgO and $I_2$ in dichloromethane,[29] or by [cobalt(II)-salen]-catalyzed oxidation using oxygen as oxidant.[30] A possible mechanism for the formation of Y–N=N–Y from the oxidation of $NH_2Y$ by $[Ru^{VI}(por)O_2]$ involves generation of reactive $[Ru^{VI}(por)(NY)_2]$ intermediate, which subsequently reacts with the arylamine and/or undergo coupling of the coordinated arylimide ligand. In this regard, we attempted to develop oxidation of $NH_2$(**Ar**–**Ar**) using $[Ru^{II}(por)(CO)]$ as a catalyst, 2,6-dichloropyridine *N*-oxide (2,6-$Cl_2$pyNO) as a terminal oxidant, and dichloromethane as solvent. However, **Ar**–**Ar**–N=N–**Ar**–**Ar** was not formed in the

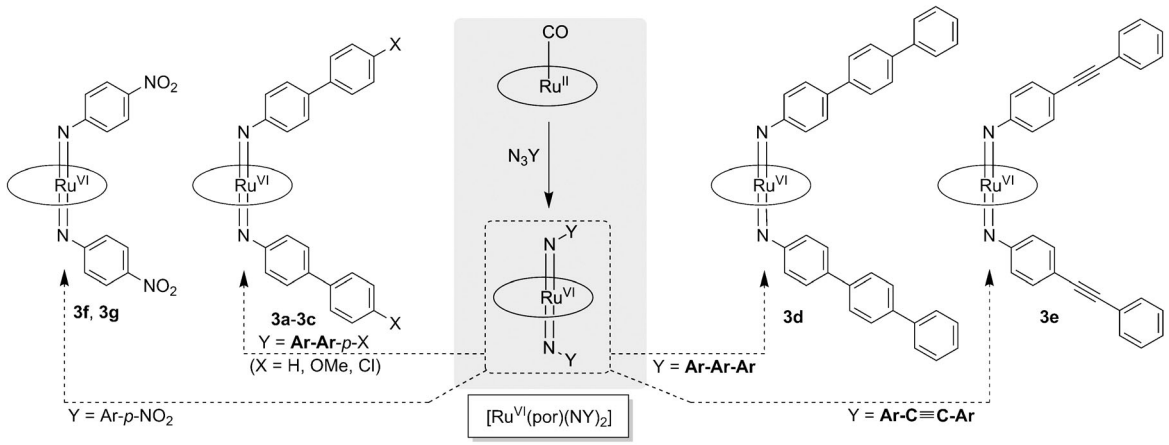


**Scheme 2.** Syntheses of $[Ru^{VI}(por)(NY)_2]$ (**3**) from reaction of $[Ru^{II}(por)(CO)]$ with $N_3Y$.

**Table 1.** Ruthenium porphyrin complexes synthesized in this work.

| Entry | Complex |
|---|---|
| $[Ru^{IV}(por)(NHY)_2]$ (**1**) | |
| 1 | $[Ru^{IV}(tmp)(NH\{\mathbf{Ar}–\mathbf{Ar}\})_2]$ (**1 a**)[a] |
| 2 | $[Ru^{IV}(tmp)(NH\{\mathbf{Ar}–\mathbf{Ar}\text{-}p\text{-}OMe\})_2]$ (**1 b**)[b] |
| 3 | $[Ru^{IV}(tmp)(NH\{\mathbf{Ar}–\mathbf{Ar}\text{-}p\text{-}Cl\})_2]$ (**1 c**)[c] |
| 4 | $[Ru^{IV}(tmp)(NH\{\mathbf{Ar}\wedge\mathbf{Ar}\})_2]$ (**1 d**)[d] |
| 5 | $[Ru^{IV}(tmp)(NH\{\mathbf{Ar}–\mathbf{Ar}–\mathbf{Ar}\})_2]$ (**1 e**)[e] |
| 6 | $[Ru^{IV}(tmp)(NH\{\mathbf{Ar}–\mathbf{C}\equiv\mathbf{C}–\mathbf{Ar}\})_2]$ (**1 f**)[f] |
| 7 | $[Ru^{IV}(tmp)(NH\{\mathbf{Ar}–\mathbf{C}\equiv\mathbf{C}–\mathbf{Ar}–\mathbf{C}\equiv\mathbf{C}–\mathbf{Ar}\})_2]$ (**1 g**)[g] |
| 8 | $[Ru^{IV}(ttp)(NH\{\mathbf{Ar}–\mathbf{Ar}\})_2]$ (**1 h**)[a] |
| 9 | $[Ru^{IV}(3,4,5\text{-OMe-tpp})(NH\{\mathbf{Ar}–\mathbf{Ar}\})_2]$ (**1 i**)[a] |
| 10 | $[Ru^{IV}(ttp)(NH\{\mathbf{Ar}\wedge\mathbf{Ar}\})_2]$ (**1 j**)[d] |
| 11 | $[Ru^{IV}(4\text{-OMe-tpp})(NH\{\mathbf{Ar}\wedge\mathbf{Ar}\})_2]$ (**1 k**)[d] |
| 12 | $[Ru^{IV}(4\text{-Cl-tpp})(NH\{\mathbf{Ar}\wedge\mathbf{Ar}\})_2]$ (**1 l**)[d] |
| 13 | $[Ru^{IV}(F_{20}\text{-tpp})(NH\{\mathbf{Ar}\wedge\mathbf{Ar}\})_2]$ (**1 m**)[d] |
| 14 | $[Ru^{IV}(tmp)(NH\{Ar\text{-}p\text{-}Cl\})_2]$ (**1 n**)[h] |
| 15 | $[Ru^{IV}(4\text{-OMe-tpp})(NH\{Ar\text{-}p\text{-}Cl\})_2]$ (**1 o**)[h] |
| $[Ru^{II}(por)(NH_2Y)_2]$ (**2**) | |
| 16 | $[Ru^{II}(F_{20}\text{-tpp})(NH_2\{\mathbf{Ar}\wedge\mathbf{Ar}\})_2]$ (**2 a**)[d] |
| 17 | $[Ru^{II}(F_{20}\text{-tpp})(NH_2\{Ar\text{-}p\text{-}Cl\})_2]$ (**2 b**)[h] |
| 18 | $[Ru^{II}(F_{20}\text{-tpp})(NH_2\{Ar\text{-}p\text{-}(NHPh)\})_2]$ (**2 c**)[i] |
| $[Ru^{VI}(por)(NY)_2]$ (**3**) | |
| 19 | $[Ru^{VI}(tmp)(N\{\mathbf{Ar}–\mathbf{Ar}\})_2]$ (**3 a**)[a] |
| 20 | $[Ru^{VI}(tmp)(N\{\mathbf{Ar}–\mathbf{Ar}\text{-}p\text{-}OMe\})_2]$ (**3 b**)[b] |
| 21 | $[Ru^{VI}(tmp)(N\{\mathbf{Ar}–\mathbf{Ar}\text{-}p\text{-}Cl\})_2]$ (**3 c**)[c] |
| 22 | $[Ru^{VI}(tmp)(N\{\mathbf{Ar}–\mathbf{Ar}–\mathbf{Ar}\})_2]$ (**3 d**)[e] |
| 23 | $[Ru^{VI}(tmp)(N\{\mathbf{Ar}–\mathbf{C}\equiv\mathbf{C}–\mathbf{Ar}\})_2]$ (**3 e**)[f] |
| 24 | $[Ru^{VI}(tmp)(N\{Ar\text{-}p\text{-}NO_2\})_2]$ (**3 f**)[j] |
| 25 | $[Ru^{VI}(ttp)(N\{Ar\text{-}p\text{-}NO_2\})_2]$ (**3 g**)[j] |
| $[Ru^{IV}(por)(NHY)Br]$ (**4**) | |
| 26 | $[Ru^{IV}(tmp)(NH\{\mathbf{Ar}–\mathbf{Ar}\})Br]$ (**4 a**)[a] |
| 27 | $[Ru^{IV}(tmp)(NH\{\mathbf{Ar}\wedge\mathbf{Ar}\})Br]$ (**4 b**)[d] |
| 28 | $[Ru^{IV}(tmp)(NH\{\mathbf{Ar}–\mathbf{Ar}–\mathbf{Ar}\})Br]$ (**4 c**)[e] |

[a] **Ar**–**Ar** = biphenyl-4-yl. [b] **Ar**–**Ar**-*p*-OMe = 4′-methoxy-biphenyl-4-yl. [c] **Ar**–**Ar**-*p*-Cl = 4′-chloro-biphenyl-4-yl. [d] **Ar**^**Ar** = 9,9-dibutyl-fluoren-2-yl. [e] **Ar**–**Ar**–**Ar** = 1,1′:4′,1″-terphenyl-4-yl. [f] **Ar**–**C**≡**C**–**Ar** = 4-(phenylethynyl)phenyl. [g] **Ar**–**C**≡**C**–**Ar**–**C**≡**C**–**Ar** = 4-((4-(phenylethynyl)phenyl)ethynyl)phenyl. [h] Ar-*p*-Cl = 4-chlorophenyl. [i] Ar-*p*-(NHPh) = 4-(phenylamino)phenyl. [j] Ar-*p*-$NO_2$ = 4-nitrophenyl.

reaction mixture as indicated by $^1$H NMR spectroscopy analysis, and > 90% of the starting $NH_2$(**Ar**–**Ar**) was recovered.

Besides oxidative deprotonation of metal–arylamine porphyrin complexes/intermediates to give $[Ru^{IV}(por)(NHY)_2]$ and $[Os^{IV}(por)(NHY)_2]$,[6a,c] other methods have also been reported for preparing/generating metal–arylamide complexes of porphyrins. $[Ti^{IV}(ttp)(NPh_2)_2]$ was prepared from reaction of $[Ti^{IV}(ttp)Cl_2]$ with $LiNPh_2$;[7a] a similar reaction of $[Hf^{IV}(ttp)Cl_2]$ with LiNH(Ar-*p*-Me) afforded $[Hf^{IV}(ttp)(NH\{Ar\text{-}p\text{-}Me\})_2]$ (Ar-*p*-Me = 4-tolyl).[7b] Treatment of $[Os^{VI}(por)O_2]$ with hydrazine gave $[Os^{IV}(por)(NPh_2)(OH)]$.[6e] The reaction of imide complexes $[M^{IV}(ttp)(N\{Ar\text{-}2,6\text{-}i\text{Pr}\})]$ (M = Zr, Hf; Ar-2,6-*i*Pr = 2,6-diisopropylphenyl) with *t*BuC(O)Me produced $[M^{IV}(ttp)(NH\{Ar\text{-}2,6\text{-}i\text{Pr}\})(OC(t\text{Bu})=CH_2)]$.[7c]

**Bis(π-conjugated arylimide) complexes**: Reaction of carbonylruthenium(II) porphyrin $[Ru^{II}(tmp)(CO)]$ with π-conjugated aryl azides $N_3Y$ (3 equiv; Y = **Ar**–**Ar**, **Ar**–**Ar**-*p*-OMe, **Ar**–**Ar**-*p*-Cl, **Ar**–**Ar**–**Ar**, **Ar**–**C**≡**C**–**Ar**) in refluxing benzene for 2 h afforded $[Ru^{VI}(tmp)(NY)_2]$ (**3**, Scheme 2; entries 19–23 in Table 1) in 60–65% yields. The unreacted aryl azides were washed away with hexane/diethyl ether, giving the $[Ru^{VI}(tmp)(NY)_2]$ in > 95% purity (by $^1$H NMR analysis).[31]

Complexes $[Ru^{VI}(tmp)(NY)_2]$ (Y = **Ar**–**Ar**, **Ar**–**Ar**-*p*-OMe, **Ar**–**Ar**-*p*-Cl) can also be generated by oxidative deprotonation reactions of the corresponding $[Ru^{IV}(tmp)(NHY)_2]$ with $PhI(OAc)_2$ (see below). In view of the formation of $[Ru^{VI}(ttp)(Nt\text{Bu})_2]$ and $[Ru^{VI}(ttp)(Nt\text{Bu})O]$ from treatment of $[Ru^{VI}(ttp)O_2]$ with *tert*-butylamine in aerobic hexane,[6d] we examined the reaction of $[Ru^{VI}(tmp)O_2]$ with $NH_2$(**Ar**–**Ar**) under similar conditions. But the latter reaction in aerobic hexane gave the same product $[Ru^{IV}(tmp)(NH\{\mathbf{Ar}–\mathbf{Ar}\})_2]$ as that in ethanol solvent; no ruthenium(VI)–arylimide species was detected.

The use of aryl azides for synthesizing metal–arylimide porphyrin complexes can be dated back to 1987, in which year the synthesis of $[Cr^{IV}(tpp)(N\{Ar\text{-}p\text{-}Me\})]$ from $N_3$(Ar-*p*-Me) and $[Cr^{II}(tpp)]$ was reported.[9a] Subsequently, $[Os^{VI}(por)(N\{Ar\text{-}p\text{-}NO_2\})_2]$ (por = ttp, 4-Cl-tpp) were synthesized from $[Os^{II}(ttp)]_2$ and $N_3$(Ar-*p*-$NO_2$), and were both structurally characterized by X-ray crystal analysis;[13] a similar reaction for $[Ru^{II}(ttp)]_2$ gave $[Ru^{VI}(tpp)(N\{Ar\text{-}p\text{-}NO_2\})_2]$.[13b] Recently, Cenini, Gallo, and their

co-workers isolated [$Ru^{VI}$(tpp)(N{Ar-3,5-$CF_3$})$_2$] by treatment of [$Ru^{II}$(tpp)(CO)] with $N_3$(Ar-3,5-$CF_3$) and determined the X-ray crystal structure of the ruthenium–bis(arylimide) complex.[8] Similar reactions of [$Ru^{II}$(por)(CO)] (por = tmp, ttp) with $N_3$(Ar-*p*-$NO_2$) in this work gave [$Ru^{VI}$(por)(N{Ar-*p*-$NO_2$})$_2$] in 60–70% yields (entries 24 and 25, Table 1). These bis(arylimide) complexes of metalloporphyrins all feature *strongly electron-withdrawing substituents on the arylimide ligands*, which would render the arylimides less susceptible to hydrolysis and thus enhance the stability of the complexes.

Notably, the bis(π-conjugated arylimide) complexes [$Ru^{VI}$(tmp)(NY)$_2$] (Y = **Ar**–**Ar**, **Ar**–**Ar**-*p*-OMe, **Ar**–**Ar**–**Ar**, **Ar**–**C**≡**C**–**Ar**) prepared in this work are *devoid of strongly electron-withdrawing groups on the arylimide ligands*. Probably, the sterically encumbered porphyrin ligand (tmp) and the electron delocalization over the π-conjugated phenyl groups play a significant role in stabilizing these bis(arylimide) complexes.

Other examples of previously reported metal–arylimide porphyrins are mono(arylimide) complexes, including [$V^{IV}$(ttp)(N{Ar-*p*-X})] (X = H, Me, OMe, Cl, *t*Bu) reported in 1985,[5b] and the subsequently reported complexes [$Cr^{IV}$(por)(N{Ar-*p*-X})] (por = tpp, X = Cl, I, OMe; por = ttp, X = Me),[9] [$Os^{VI}$(por)(N{Ar-*p*-F})(O)] (por = tpp, 3,4,5-OMe-tpp),[6a,c] [$Ti^{IV}$(ttp)(N{Ar-*p*-X})] (X = H, Me),[7a, 10a,b] [$Ru^{IV}$(por)(N{Ar-*p*-X})] (por = tbpp, X = H, Me, Cl, I; por = ttp, X = Me),[11] [$M^{IV}$(ttp)(N{Ar-2,6-*i*Pr})] (M = Zr, Hf),[7b] [$Mo^{IV}$(ttp)(NY)] (Y = Ph, Ar-*p*-Me, Ar-2,4,6-Me, Ar-2,6-*i*Pr),[10c] and [$V^{IV}$(oep)(NPh)].[12] These complexes were prepared by reactions of M–Cl (M = V, Ti, Ru) complexes with $NH_2Y$[5b, 11, 12] or LiNHY,[7a, b, 10a,c] reactions of [$Cr^{II}$(por)] with aryl azides,[9] or autoxidation of Os–NHY complexes.[6a,c]

## Stability

The complexes [$Ru^{IV}$(por)(NHY)$_2$] and [$Ru^{VI}$(por)(NY)$_2$] prepared in this work (Table 1) are soluble in chloroform and dichloromethane. Of these complexes, [$Ru^{IV}$(por)(NHY)$_2$] are stable toward air and moisture for more than one month in the solid state and for about one week in aerobic chloroform or dichloromethane solutions; [$Ru^{VI}$(por)(NY)$_2$] are stable for serveral hours in chloroform solutions and for about 1 day in the solid state (all at room temperature). Upon standing the solutions for days, [$Ru^{VI}$(por)(NY)$_2$] was reduced to [$Ru^{IV}$(por)(NHY)$_2$] and decomposed to some unknown species.

## Spectroscopy

**$^1$H NMR spectroscopy**: The [$Ru^{IV}$(por)(NHY)$_2$], [$Ru^{VI}$(por)(NY)$_2$], and [$Ru^{II}$(por)($NH_2$Y)$_2$] (Table 1) all show diamagnetic $^1$H NMR spectra. The signals of porphyrin pyrrolic protons, $H_\beta$, appear at $\delta$ = 8.16–8.57 ppm for [$Ru^{IV}$(por)(NHY)$_2$] (Table S1 in the Supporting Information; NH signals not located)[6d] and at $\delta$ = 8.53–8.84 ppm for [$Ru^{VI}$(por)(NY)$_2$] (Table S2 in the Supporting Information).

The spectra of [$Ru^{IV}$(tmp)(NH{**Ar**–**Ar**})$_2$] and [$Ru^{VI}$(tmp)(N{**Ar**–**Ar**})$_2$], as examples, are shown in Figure 2. Both spectra have the following features: 1) the intensity ratio of signals corresponds to a 1:2 molar ratio of tmp versus axial ligand; 2) there is only a single set of **Ar**–**Ar** signals, indicating that the two axially coordinated arylamide or arylimide ligands are equivalent; 3) for the **Ar**–**Ar** group, the phenyl moiety closer to the porphyrin ring gives more separated and upfield-shifted signals ($H_o'$ and $H_m'$ in Figure 2 at $\delta \approx 3$ and 6 ppm, respectively) due to a larger effect of the porphyrin ring current; the other phenyl moiety exhibits much less separated signals at $\delta \approx 7$ ppm ($H_o''$, $H_m''$, $H_p''$ in Figure 2). Compared with the **Ar**–**Ar** signals of [$Ru^{IV}$(tmp)(NH{**Ar**–**Ar**})$_2$] ($\delta$ = 7.14–6.99, 6.03, 3.28 ppm), those of [$Ru^{VI}$(tmp)(N{**Ar**–**Ar**})$_2$] ($\delta$ = 7.08–6.82, 5.94, 2.86 ppm) are upfield-shifted, in agreement with the shorter Ru–N(arylimide) than Ru–N(arylamide) distances (see below).

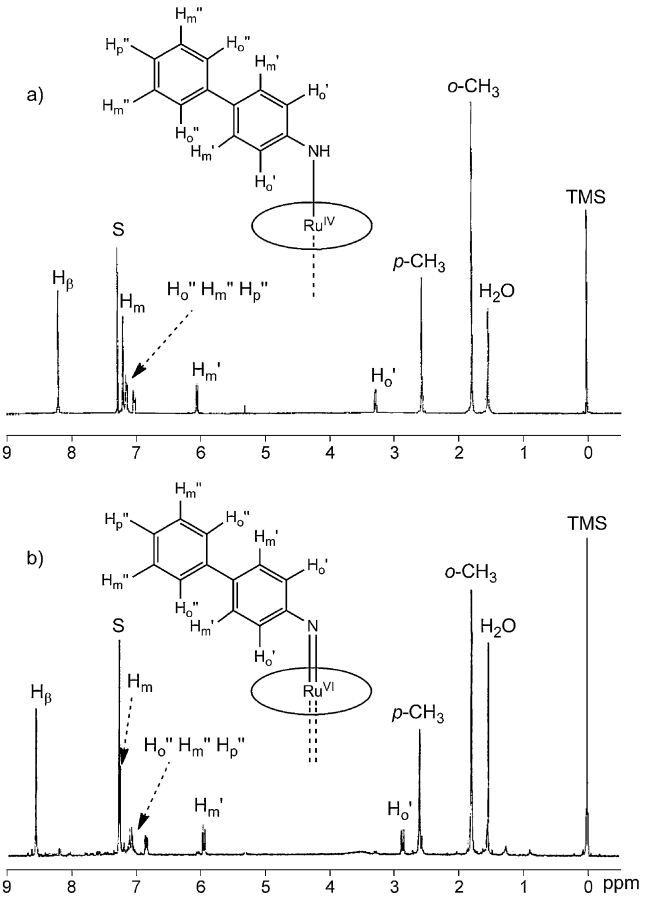


**Figure 2.** $^1$H NMR spectra (300 MHz) of: a) [$Ru^{IV}$(tmp)(NH{**Ar**–**Ar**})$_2$] (**1 a**), and b) [$Ru^{VI}$(tmp)(N{**Ar**–**Ar**})$_2$] (**3 a**) in $CDCl_3$. The tmp signals are labeled by $H_\beta$ (pyrrolic protons), $H_m$ (*m*-H of the 5,10,15,20-mesityl groups), *o*-$CH_3$, and *p*-$CH_3$. The arylamide/arylimide $H_o'$ and $H_m'$ signals were assigned by comparison with the $^1$H NMR spectra of [$Ru^{IV}$(ttp)(NH{Ar-*p*-X})$_2$][6d] and [$Ru^{VI}$(tpp)(N{Ar-*p*-$NO_2$})$_2$].[13b]

Complexes [$Ru^{IV}$(tmp)(NHY)$_2$] (Y = **Ar**–**Ar**, **Ar**–**Ar**-*p*-OMe, **Ar**–**Ar**-*p*-Cl, **Ar**^**Ar**, **Ar**–**Ar**–**Ar**, **Ar**–**C**≡**C**–**Ar**, **Ar**–**C**≡**C**–**Ar**–**C**≡**C**–**Ar**, Ar-*p*-Cl) exhibit $H_\beta$ signals with similar chemical shifts ($\delta$ = 8.16–8.19 ppm). The $H_\beta$ chemical shifts of [$Ru^{VI}$(tmp)(NY)$_2$] (Y = **Ar**–**Ar**, **Ar**–**Ar**-*p*-OMe, **Ar**–**Ar**-*p*-Cl, **Ar**–**Ar**–**Ar**, **Ar**–**C**≡**C**–**Ar**) are also similar ($\delta$ = 8.53–8.56 ppm), though slightly smaller than that of [$Ru^{VI}$(tmp)(N{Ar-*p*-$NO_2$})$_2$] ($\delta$ = 8.64 ppm). This shows that the various π-conjugated aryl groups have a similar effect on the pyrrolic proton resonances despite the different extent of π conjugation.

More significant variation of $H_\beta$ chemical shifts was observed among different types of porphyrin ligands, with $\delta = 8.17$–8.43 ppm for $[Ru^{IV}(por)(NH\{\mathbf{Ar}\text{^}\mathbf{Ar}\})_2]$ (por = tmp, ttp, 4-OMe-tpp, 4-Cl-tpp, $F_{20}$-tpp), $\delta = 8.17$–8.57 ppm for $[Ru^{IV}(por)(NH\{\mathbf{Ar}\text{–}\mathbf{Ar}\})_2]$ (por = tmp, ttp, 3,4,5-OMe-tpp), and $\delta = 8.64$–8.84 ppm for $[Ru^{VI}(por)(N\{Ar\text{-}p\text{-}NO_2\})_2]$ (por = tmp, ttp).

Comparison of the $H_\beta$ chemical shifts of $[Ru^{IV}(tmp)(NH\{\mathbf{Ar}\text{–}\mathbf{Ar}\})_2]$ ($\delta = 8.17$ ppm) and $[Ru^{VI}(tmp)(N\{\mathbf{Ar}\text{–}\mathbf{Ar}\})_2]$ ($\delta = 8.55$ ppm) indicates that the $H_\beta$ protons of the latter are more greatly deshielded, consistent with the higher oxidation state of Ru in $[Ru^{VI}(por)(NY)_2]$ than in $[Ru^{IV}(por)(NHY)_2]$.[32] However, compared with $[Ru^{VI}(tmp)O_2]$, which shows $H_\beta$ signal at $\delta = 8.81$ ppm,[33] $[Ru^{VI}(tmp)(N\{\mathbf{Ar}\text{–}\mathbf{Ar}\})_2]$ exhibits less deshielded $H_\beta$ protons, suggesting that the arylimide ligand is a better $\pi$ donor than the oxo ligand.

As expected, the $H_\beta$ signals of $[Ru^{II}(F_{20}\text{-tpp})(NH_2Y)_2]$ (Y = **Ar^Ar**, Ar-*p*-Cl, Ar-*p*-(NHPh)) ($\delta = 8.03$–8.07 ppm) are considerably upfield from that of $[Ru^{IV}(F_{20}\text{-tpp})(NH\{\mathbf{Ar}\text{^}\mathbf{Ar}\})_2]$ ($\delta = 8.41$ ppm). It is worth noting that $NH_2$(Ar-*p*-(NHPh)) has two amino groups that can be deprotonated, unlike the other arylamines used in this work. While $[Ru^{II}(F_{20}\text{-tpp})(NH_2\{Ar\text{-}p\text{-}(NHPh)\})_2]$ was obtained from the reaction of $[Ru^{VI}(F_{20}\text{-tpp})O_2]$ with $NH_2$(Ar-*p*-(NHPh)), change of $[Ru^{VI}(F_{20}\text{-tpp})O_2]$ to $[Ru^{VI}(por)O_2]$ (por = tmp, 4-Cl-tpp) for this reaction resulted in the formation of a mixture of products featuring three $H_\beta$ signals: $\delta = 8.15$, 8.13, 8.11 ppm (intensity ratio: 1.2:2.2:1.0) for por = tmp; $\delta = 8.37$, 8.35, 8.33 ppm (intensity ratio: 1.8:2.6:1.0) for por = 4-Cl-tpp, which can be attributed to complexes $[Ru^{IV}(por)(NH\{Ar\text{-}p\text{-}(NHPh)\})_2]$, $[Ru^{IV}(por)(N(Ph)\{Ar\text{-}p\text{-}NH_2\})_2]$, and $[Ru^{IV}(por)(NH\{Ar\text{-}p\text{-}(NHPh)\})(N(Ph)\{Ar\text{-}p\text{-}NH_2\})]$ (Figure S1 in the Supporting Information).[34]

**UV/Vis and IR**: Complexes $[Ru^{IV}(por)(NHY)_2]$ in Table 1 exhibit UV/Vis spectra which feature the Soret bands at 412–419 nm and $\beta$ bands at 522–533 nm, similar to those (Soret: 413–417 nm, $\beta$: 527–529 nm) reported for $[Ru^{IV}(por)(NH\{Ar\text{-}p\text{-}X\})_2]$ (por = ttp, 4-Cl-tpp; X = Cl, $NO_2$).[6d] $[Ru^{II}(F_{20}\text{-tpp})(NH_2Y)_2]$ (Y = **Ar^Ar**, Ar-*p*-Cl, Ar-*p*-(NHPh)) gave Soret and $\beta$ bands at 401–403 and 501–502 nm, respectively; these bands are markedly blue-shifted from the corresponding bands of $[Ru^{IV}(F_{20}\text{-tpp})(NH\{\mathbf{Ar}\text{^}\mathbf{Ar}\})_2]$ (Soret: 412 nm, $\beta$: 522 nm).

$[Ru^{VI}(por)(NY)_2]$ in Table 1 exhibit Soret bands at 417–423 nm and $\beta$ bands at 526–530 nm. Conversion of $[Ru^{II}(tmp)(CO)]$ to, for example, $[Ru^{VI}(tmp)(N\{\mathbf{Ar}\text{^}\mathbf{Ar}\})_2]$ resulted in a red shift of the Soret band from 412 to 423 nm; the latter is also red-shifted from that of $[Ru^{IV}(tmp)(NH\{\mathbf{Ar}\text{–}\mathbf{Ar}\})_2]$ (Soret: 418 nm).

For $[Ru^{VI}(tmp)(NY)_2]$ bearing various axial arylimide ligands, the effects of aryl groups of the arylimide ligands on the Soret/$\beta$ bands of these complexes are similar (Soret: 421–423 nm, $\beta$: 526–529 nm). A similar phenomenon was observed for the effect of aryl groups of the axial arylamide ligands in $[Ru^{IV}(tmp)(NHY)_2]$ on their Soret (416–419 nm) and $\beta$ (526–528 nm) bands.

The IR spectra of the $[Ru^{IV}(por)(NHY)_2]$ in Table 1 show a $\nu$(NH) band at 3254–3269 $cm^{-1}$, similar to those reported for $[Ru^{IV}(por)(NH\{Ar\text{-}p\text{-}X\})_2]$ (por = ttp, 4-Cl-tpp; X = Cl, $NO_2$: $\nu$(NH) at 3264–3267 $cm^{-1}$).[6d] $[Ru^{II}(F_{20}\text{-tpp})(NH_2Y)]$ (Y = **Ar^Ar**, Ar-*p*-Cl, Ar-*p*-(NHPh)) each shows two $\nu$(NH) bands in the region of 3262–3403 $cm^{-1}$. Similar $\nu$(NH) bands are not present in the IR spectra of the $[Ru^{VI}(por)(NY)_2]$ complexes.

### X-ray crystal structures

Diffraction-quality crystals were obtained for $[Ru^{IV}(tmp)(NHY)_2]$ with Y = **Ar**–**Ar**-*p*-OMe, **Ar**–**Ar**-*p*-Cl, and **Ar^Ar** and for $[Ru^{VI}(tmp)(N\{\mathbf{Ar}\text{–}\mathbf{Ar}\text{-}p\text{-}OMe\})_2]$. The structures of these complexes determined by X-ray crystallography[35] are depicted in Figures 3–5 and Figure S2 in the Supporting Information, and the crystallographic data and selected bond lengths and angles are listed in Tables S3–S6 in the Supporting Information. For previously reported $[V^{IV}(ttp)(N\{\mathbf{Ar}\text{–}\mathbf{Ar}\})]$[5b] mentioned in the Introduction section, its crystal structure remains to be determined, although $[V^{IV}(oep)(NPh)]$ has been structurally characterized recently.[12]

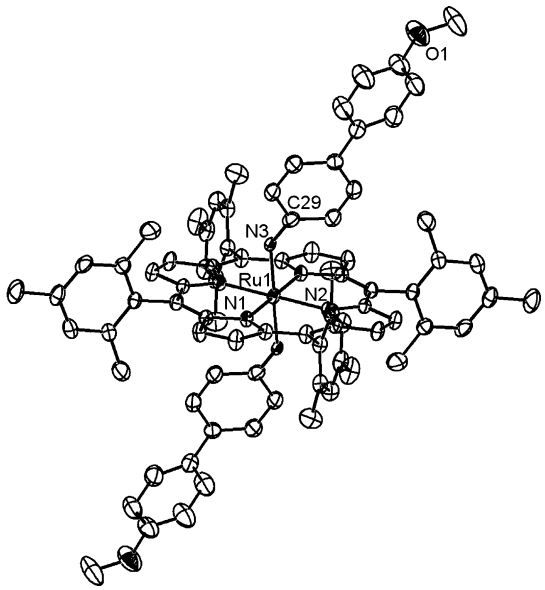


**Figure 3.** ORTEP drawing for $[Ru^{IV}(tmp)(NH\{\mathbf{Ar}\text{–}\mathbf{Ar}\text{-}p\text{-}OMe\})_2]$ (**1b**, thermal ellipsoids at 30% probability; hydrogen atoms are omitted). Ru1–N3 1.978(4) Å, Ru1-N3-C29 141.9(3)°.

Complexes $[Ru^{IV}(tmp)(NHY)_2]$ show Ru–N(arylamide) distances of 1.978(4), 1.971(6), and 1.985(13) Å for Y = **Ar**–**Ar**-*p*-OMe, **Ar**–**Ar**-*p*-Cl, and **Ar^Ar**, with axial Ru-N-C angles of 141.9(3)°, 139.3(6)°, and 136.1(9)°, respectively, which are comparable to the corresponding geometrical parameters (1.956(7) Å and 135.8(6)°) reported for $[Ru^{IV}(ttp)(NH\{Ar\text{-}p\text{-}Cl\}_2]$.[6d] These Ru–N(arylamide) distances (1.956(7)–1.985(13) Å) are substantially shorter than the Ru–N(amine) distance in $[Ru^{II}(tmp)(NH_2CH_2Ph)_2]$ (2.129 Å),[23] revealing the multiple-bonding character of the Ru–N(arylamide) bonds in the $[Ru^{IV}(por)(NHY)_2]$ complexes.

$[Ru^{IV}(tmp)(NH\{\mathbf{Ar}\text{^}\mathbf{Ar}\})_2]$ features a unique arylamide ligand in which the two mutually conjugated phenyl rings are coplanar, thus maximizing the through resonance between these phenyl groups (Figure 4). Changing the aryl group from **Ar^Ar**

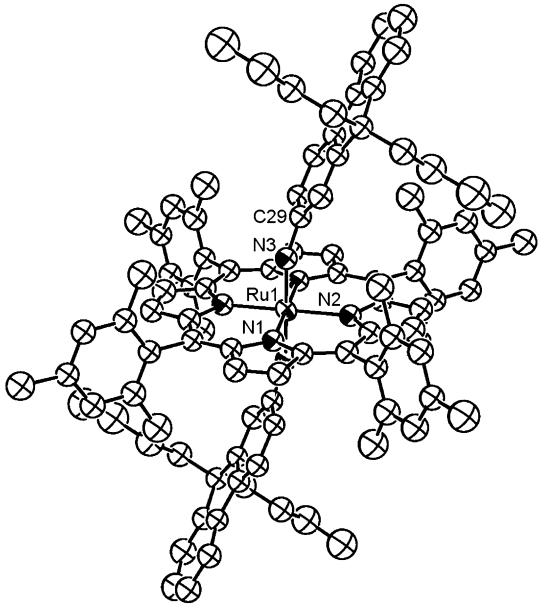


**Figure 4.** ORTEP drawing for [Ru$^{IV}$(tmp)(NH{**Ar**^**Ar**})$_2$] (**1 d**, thermal ellipsoids at 30% probability; hydrogen atoms are omitted). Ru1–N3 1.985(13) Å, Ru1-N3-C29 136.9(3)°.

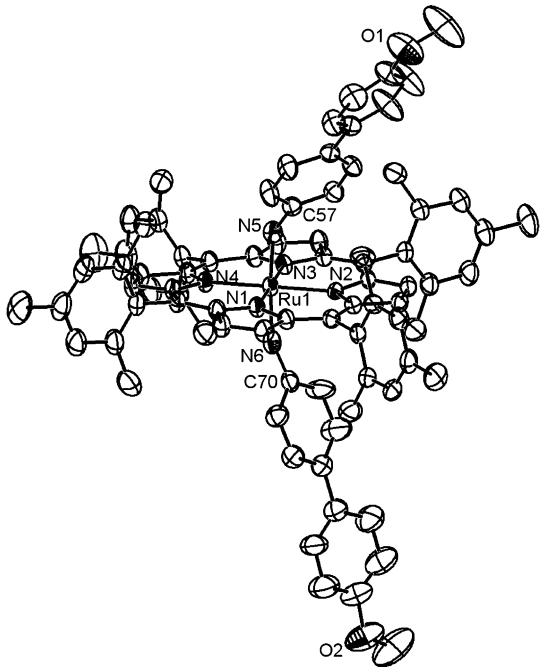


**Figure 5.** ORTEP drawing for [Ru$^{VI}$(tmp)(N{**Ar**–**Ar**-*p*-OMe})$_2$] (**3 b**, thermal ellipsoids at 30% probability; hydrogen atoms are omitted). Ru1–N5 1.829(5), Ru1–N6 1.824(5) Å; Ru1-N5-C57 136.9(3)°, Ru1-N6-C70 153.5(4)°, N5-Ru1-N6 172.8(2)°.

to **Ar**–**Ar**-*p*-OMe and **Ar**–**Ar**-*p*-Cl results in appreciable distortion of the two phenyl groups from co-planarity. For example, a dihedral angle of 24.5° is observed for the two phenyl rings in each **Ar**–**Ar**-*p*-OMe group of [Ru$^{IV}$(tmp)(NH{**Ar**–**Ar**-*p*-OMe})$_2$]. Such distortion does not significantly alter the Ru–N(arylamide) distances in the complex. In the crystal structure of non-porphyrin *cis*-bis(arylamide) complex [Lu(*t*Bu$_3${2′-Me$_3$SiCH$_2$}tpy)(NH{**Ar**–**Ar**-3,5-Ph})$_2$] (tpy = 2,2′:6′,2″-terpyridine; **Ar**–**Ar**-3,5-Ph = 3,5-diphenyl-biphenyl-4-yl),[4b] the two phenyl rings of the biphenyl moiety of **Ar**–**Ar**-3,5-Ph make larger dihedral angles of 35.3° and 43.7°.

For [Ru$^{VI}$(tmp)(N{**Ar**–**Ar**-*p*-OMe})$_2$], its Ru–N(arylimide) distances of 1.824(5), 1.829(5) Å and axial Ru-N-C angles of 136.9(3)°, 153.5(4)° are comparable to those reported for [Ru$^{VI}$(tpp)(N{Ar-3,5-CF$_3$})$_2$] (1.808(4), 1.806(4) Å; 139.8(3)°, 143.7(4)°; Figure 5).[8] These two [Ru$^{VI}$(por)(NY)$_2$] complexes show similar orientation of the axial arylimide ligands with respect to the corresponding porphyrin ring. Their Ru–N(imide) distances are comparable to, and the axial imide ligands are more bent than, those of the sulfonylimide analogue [Ru$^{VI}$(tmp)(NSO$_2${Ar-*p*-OMe})$_2$] (Ru–N(imide) 1.79(3) Å, axial Ru-N-S: 162.5(3)°).[36]

Comparison of the structures between [Ru$^{VI}$(tmp)(N{**Ar**–**Ar**-*p*-OMe})$_2$] and [Ru$^{IV}$(tmp)(NH{**Ar**–**Ar**-*p*-OMe})$_2$] revealed the following differences. 1) The Ru–N(arylimide) distances (1.824(5), 1.829(5) Å) are considerably shorter than the Ru–N(arylamide) distance (1.978(4) Å), in line with the larger character of Ru–N multiple bonding anticipated for Ru–imide than Ru–amide complex. 2) The dihedral angle between the two phenyl rings of the **Ar**–**Ar**-*p*-OMe group in the arylimide complex (16.3°, 16.9°) is smaller than that in the arylamide complex (24.5°), suggesting a higher extent of π conjugation in the former case. 3) The axial N-Ru-N axis is slightly bent (with an angle of 172.8(2)°) in the arylimide complex, but is linear (with an angle

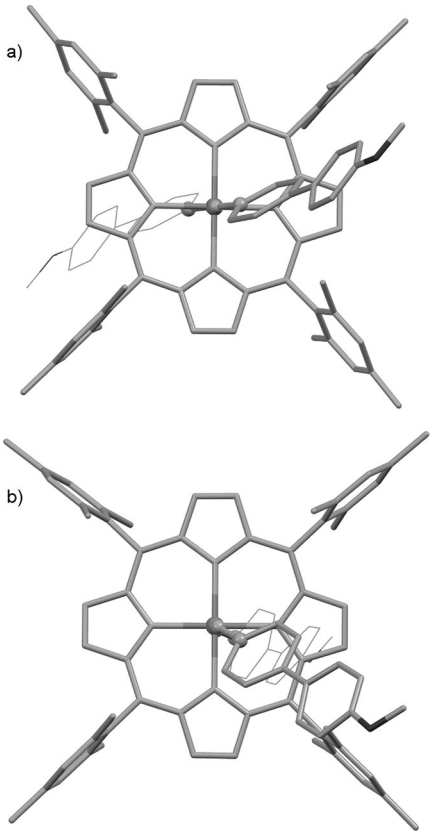


**Figure 6.** Top-views of: a) [Ru$^{IV}$(tmp)(NH{**Ar**–**Ar**-*p*-OMe})$_2$] (**1 b**, along N3···N3′ axis), and b) [Ru$^{VI}$(tmp)(N{**Ar**–**Ar**-*p*-OMe})$_2$] (**3 b**, along N5···N6 axis). The axial C–N–Ru–N–C moiety is in ball-and-stick representation, whereas the **Ar**–**Ar**-*p*-OMe group behind the porphyrin plane is in wire frame representation.

of 180°) in the arylamide counterpart. 4) The two axial arylimide ligands adopt a *syn* configuration, in contrast to the *anti* configuration of the two axial arylamide ligands (Figure 6).

### Electrochemistry

The cyclic voltammograms of several $[Ru^{IV}(tmp)(NHY)_2]$ complexes in dichloromethane were measured. The cyclic voltammogram of $[Ru^{IV}(tmp)(NH\{\mathbf{Ar}–\mathbf{C}\equiv\mathbf{C}–\mathbf{Ar}–\mathbf{C}\equiv\mathbf{C}–\mathbf{Ar}\})_2]$ as an example, in which a total of six waves, **I**–**IV** and **I**′/**II**′, were observed, is shown in Figure 7. Both the reduction wave **III** and

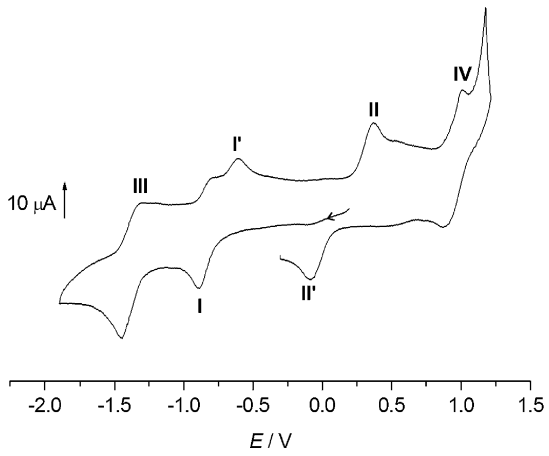


**Figure 7.** Cyclic voltammogram of $[Ru^{IV}(tmp)(NH\{\mathbf{Ar}–\mathbf{C}\equiv\mathbf{C}–\mathbf{Ar}–\mathbf{C}\equiv\mathbf{C}–\mathbf{Ar}\})_2]$ (**1 g**) in $CH_2Cl_2$ at 25 °C. Scan rate: 100 mV $s^{-1}$.

the oxidation wave **IV** are reversible; the reduction wave **I** is quasi-reversible, and the other waves are irreversible. The irreversible waves **I**′ and **II**′ are attributed to the species generated by reduction **I** and oxidation **II**, respectively, since neither wave **I**′ is present prior to reduction **I**, nor is wave **II**′ before oxidation **II**. A collection of the potentials of waves **I**–**IV** for the $[Ru^{IV}(tmp)(NHY)_2]$ complexes examined are listed in Table 2.

The potentials of the reversible oxidation couples **IV** ($E_{1/2}$ = 0.68–0.78 V vs. $Cp_2Fe^{+/0}$, Table 2) are comparable to those of the porphyrin-centered oxidation reported for $[Ru^{II}(tmp)(CO)]$ (0.86 V),[37] $[Ru^{VI}(tmp)(NSO_2\{Ar\text{-}p\text{-}X\})_2]$ (X = OMe, Me, H, Cl, $NO_2$: 0.61–0.75 V),[15d] and $[Ru^{VI}(tmp)O_2]$ (0.69 V),[38] revealing a porphyrin-centered oxidation. For the reversible reduction couples **III** at $E_{1/2}$ = −1.54 to −1.78 V, their potentials are comparable to those of the porphyrin-centered reduction of the above $Ru^{VI}$ complexes ($E_{1/2}$ = −1.46 to −1.61 V).[15d]

**Table 2.** Redox potentials ($E$ vs. $Cp_2Fe^{+/0}$) of $[Ru^{IV}(tmp)(NHY)_2]$ (**1**).

| $[Ru^{IV}(tmp)(NHY)_2]$ Y | **III** $E_{1/2}$ [V] | **I** $E_{pc}$ [V] | **II** $E_{pa}$ [V] | **IV** $E_{1/2}$ [V] |
|---|---|---|---|---|
| **Ar^Ar** (**1 d**) | – | −1.40 | −0.044 | 0.68 |
| **Ar–Ar**-*p*-OMe (**1 b**) | – | −1.32 | 0.048 | – |
| **Ar–Ar–Ar** (**1 e**) | −1.59 | −1.25 | 0.094 | 0.73 |
| **Ar–Ar** (**1 a**) | – | −1.24 | 0.12 | – |
| **Ar–Ar**-*p*-Cl (**1 c**) | −1.78 | −1.23 | 0.15 | 0.78 |
| **Ar–C≡C–Ar** (**1 f**) | – | −1.11 | 0.19 | – |
| **Ar–C≡C–Ar–C≡C–Ar** (**1 g**) | −1.54 | −1.06 | 0.19 | 0.78 |

The quasi-reversible/irreversible reduction waves **I** have $E_{pc}$ values in the range of −1.06 to −1.40 V and the $E_{pa}$ values of the irreversible oxidation waves **II** are in the range of −0.044 to 0.19 V (vs. $Cp_2Fe^{+/0}$, Table 2). We assign these reduction and oxidation processes to $Ru^{IV}\rightarrow Ru^{III}$ and $Ru^{IV}\rightarrow Ru^{V}$, respectively, owing to the following features of the $E_{pc}$ (wave **I**) and $E_{pa}$ (wave **II**) values: 1) they are substantially different from those of the porphyrin-centered reduction/oxidation;[39] 2) they are less sensitive to the substituent on the aryl group of the coordinated arylamide ligand. For example, the $E_{pc}(Ru^{IV/III})/E_{pa}(Ru^{V/IV})$ values of $[Ru^{IV}(tmp)(NHY)_2]$ are −1.32/+0.048 V for Y = **Ar–Ar**-*p*-OMe and −1.23/+0.15 V for Y = **Ar–Ar**-*p*-Cl. By changing the aryl group of $[Ru^{IV}(tmp)(NHY)_2]$ from **Ar^Ar** to **Ar–C≡C–Ar–C≡C–Ar**, the $E_{pc}(Ru^{IV/III})$ and $E_{pa}(Ru^{V/IV})$ can be tuned by 340 and 234 mV, respectively.

### DFT calculations: electronic structure of $[Ru^{VI}(por)(NY)_2]$

We studied the electronic structure of $[Ru^{VI}(por)(NY)_2]$ by density functional theory (DFT) calculations, using model complex $[Ru^{VI}(tmp)(N\{\mathbf{Ar}–\mathbf{Ar}\text{-}p\text{-}OH\})_2]$. The geometrical parameters of the DFT-optimized structure of this model complex (Figure 8) agree well with those of the crystal structure of $[Ru^{VI}(tmp)(N\{\mathbf{Ar}–\mathbf{Ar}\text{-}p\text{-}OMe\})_2]$ (Table 3).

The computed molecular orbital (MO) diagram is depicted in Figure 9. HOMO and HOMO−2 are nonbonding orbitals of $N(p_x,p_y)$ of the arylimide ligand, whereas LUMO and LUMO+1 are antibonding orbitals involving N(imide) and Ru $d_{yz}$ or $d_{xz}$ orbitals, respectively. HOMO−1 and HOMO−3 are porphyrin-based orbitals; HOMO−5 is nonbonding Ru $d_{xy}$ orbital. HOMO−29 is the π-bonding oribtal between π oribtals of

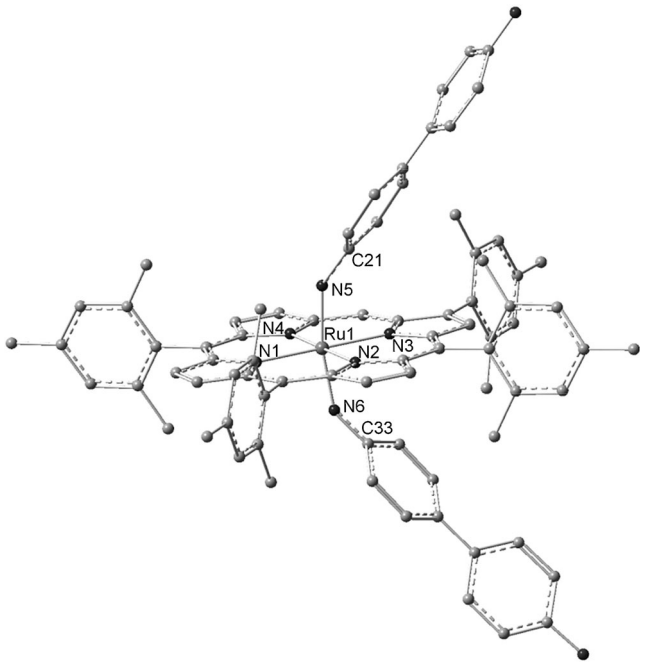


**Figure 8.** DFT-optimized structure of $[Ru^{VI}(tmp)(N\{\mathbf{Ar}–\mathbf{Ar}\text{-}p\text{-}OH\})_2]$ (hydrogen atoms are not shown).

**Table 3.** Selected bond distances [Å] and angles [°] obtained by DFT calculations and experimental studies.

| | $[Ru^{VI}(tmp)(N\{\mathbf{Ar}–\mathbf{Ar}\text{-}p\text{-}OH\})_2]$ (calcd) | $[Ru^{VI}(tmp)(N\{\mathbf{Ar}–\mathbf{Ar}\text{-}p\text{-}OMe\})_2]$ (**3b**, exptl)[a] |
|---|---|---|
| Ru1-N5 | 1.831 | 1.829(5) |
| Ru1-N6 | 1.832 | 1.824(5) |
| Ru1-N1 | 2.063 | 2.061(4) |
| Ru1-N2 | 2.097 | 2.066(3) |
| Ru1-N3 | 2.101 | 2.059(4) |
| Ru1-N4 | 2.075 | 2.055(4) |
| N5-C21[b] | 1.340 | 1.373(7) |
| N6-C33[b] | 1.340 | 1.341(7) |
| Ru1-N5-C21[b] | 145.6 | 145.5(4) |
| Ru1-N6-C33[b] | 145.5 | 153.5(4) |
| N5-Ru1-N6 | 169.0 | 172.8(2) |
| DA[b,c] | −0.3 | −14.6(7) |

[a] Data from the X-ray crystal structure. [b] The C21 or C33 atom here for $[Ru^{VI}(tmp)(N\{\mathbf{Ar}–\mathbf{Ar}\text{-}p\text{-}OMe\})_2]$ corresponds to the C57 or C70 atom, respectively, in Figure 5. [c] DA: C21-N5-N6-C33 torsion angle.

N(imide) and $d_\pi$ orbitals of Ru. This MO diagram indicates a singlet ground state consistent with a $d^2$ $Ru^{VI}$ formulation, which accounts for the related spectral features (such as the diamagnetic $^1H$ NMR spectra of $[Ru^{VI}(por)(NY)_2]$ with larger $H_\beta$ chemical shifts than those of $[Ru^{IV}(por)(NHY)_2]$) described above.

As revealed from the frontier MOs (Figure 9), there is extensive delocalization of the electron density over the whole YN=Ru=NY axial moiety, and the delocalization becomes more prominent in the HOMO.

The computed C-$N_{imide}$-$N_{mide}$-C torsion angle of −0.3° (C21-N5-N6-C33, Table 3) is close to 0° and is comparable to those in the crystal structures of $[Ru^{VI}(tmp)(N\{\mathbf{Ar}–\mathbf{Ar}\text{-}p\text{-}OMe\})_2]$ (−14.6°) and previously reported $[Ru^{VI}(tpp)(N\{Ar\text{-}3,5\text{-}CF_3\})_2]$[8] (5.7°), $[Os^{VI}(ttp)(N\{Ar\text{-}p\text{-}NO_2\})_2]$[13a] (−2.5°) and $[Os^{VI}(4\text{-}Cl\text{-}tpp)(N\{Ar\text{-}p\text{-}NO_2\})_2]$[13b] (−5.9°). In contrast, a large C-$N_{amide}$-$N_{amide}$-C torsion angle of 180° has been found in the DFT-optimized structure of $[Ru^{IV}(por^0)(NHPh)_2]$ reported previously[40] and in the crystal structure of $[Ru^{IV}(tmp)(NH\{\mathbf{Ar}–\mathbf{Ar}\text{-}p\text{-}OMe\})_2]$. The C-$N_{amide}$-$N_{amide}$-C torsion angle for the structurally characterized $[Ru^{IV}(ttp)(NH\{Ar\text{-}p\text{-}Cl\})_2]$ (~136°)[6d] is also large though considerably deviated from 180° due possibly to crystal packing effect. The computed C-$N_{amide}$-$N_{amide}$-C[40] and C-$N_{imide}$-$N_{mide}$-C torsion angles are in accord with the *anti* configuration of $[Ru^{IV}(por)(NHY)_2]$ but the *syn* configuration of $[Ru^{VI}(por)(NY)_2]$ revealed by X-ray crystal structure determinations (see, for example, Figure 6).

The $N_{imide}$-Ru-$N_{imide}$ axis is appreciably bent in both the DFT-optimized structure of $[Ru^{VI}(tmp)(N\{\mathbf{Ar}–\mathbf{Ar}\text{-}p\text{-}OH\})_2]$ and the crystal structure of $[Ru^{VI}(tmp)(N\{\mathbf{Ar}–\mathbf{Ar}\text{-}p\text{-}OMe\})_2]$ (N5-Ru1-N6 angle: 169.0° and 172.8(2)°, respectively; Table 3), with the two *trans* arylimide ligands bending to the same side to give the *syn* configuration. A similar *syn* configuration with an appreciably bent $N_{imide}$-M-$N_{imide}$ axis has also been found for the previously reported crystal structures of several $d^2$ metal–bis(arylimide) porphyrins including $[Ru^{VI}(tpp)(N\{Ar\text{-}3,5\text{-}CF_3\})_2]$,[8] $[Os^{VI}(ttp)(N\{Ar\text{-}p\text{-}NO_2\})_2]$,[13a] and $[Os^{VI}(4\text{-}Cl\text{-}tpp)(N\{Ar\text{-}p\text{-}NO_2\})_2]$[13b] ($N_{imide}$-M-$N_{imide}$ angles: 165.1(2)°–167.97(18)°). This is different from the linear $N_{amide}$-Ru-$N_{amide}$ axis (with an angle of 180°) in the DFT-optimized structure of $[Ru^{IV}(por^0)(NHPh)_2]$[40] and the crystal structure of $[Ru^{IV}(tmp)(NH\{\mathbf{Ar}–\mathbf{Ar}\text{-}p\text{-}OMe\})_2]$ both with *anti* configuration.

For $[Ru^{VI}(tmp)(N\{\mathbf{Ar}–\mathbf{Ar}\text{-}p\text{-}OH\})_2]$, the N5/N6 orbital used for the π-bonding of $N_{imide}$–Ru–$N_{imide}$ (N5–Ru1/N6–Ru1) has 4.3% s orbital and 95.7% p orbital characters (from NBO analysis). We further performed DFT calculations on the structurally characterized $[Ru^{VI}(tpp)(N\{Ar\text{-}3,5\text{-}CF_3\})_2]$,[8] $[Os^{VI}(ttp)(N\{Ar\text{-}p\text{-}NO_2\})_2]$,[13a] and $[Os^{VI}(4\text{-}Cl\text{-}tpp)(N\{Ar\text{-}p\text{-}NO_2\})_2]$,[13b] which gave geometrical parameters in good agreement with those in their crystal structures (Table S7 in the Supporting Information) and revealed similar s orbital characters of 6.6, 7.5, and 7.5%, respectively, in the corresponding N(imide) (N5/N6) orbital used for the $N_{imide}$–M–$N_{imide}$ π-bonding. We suggest that, for these metal–bis(arylimide) complexes, the

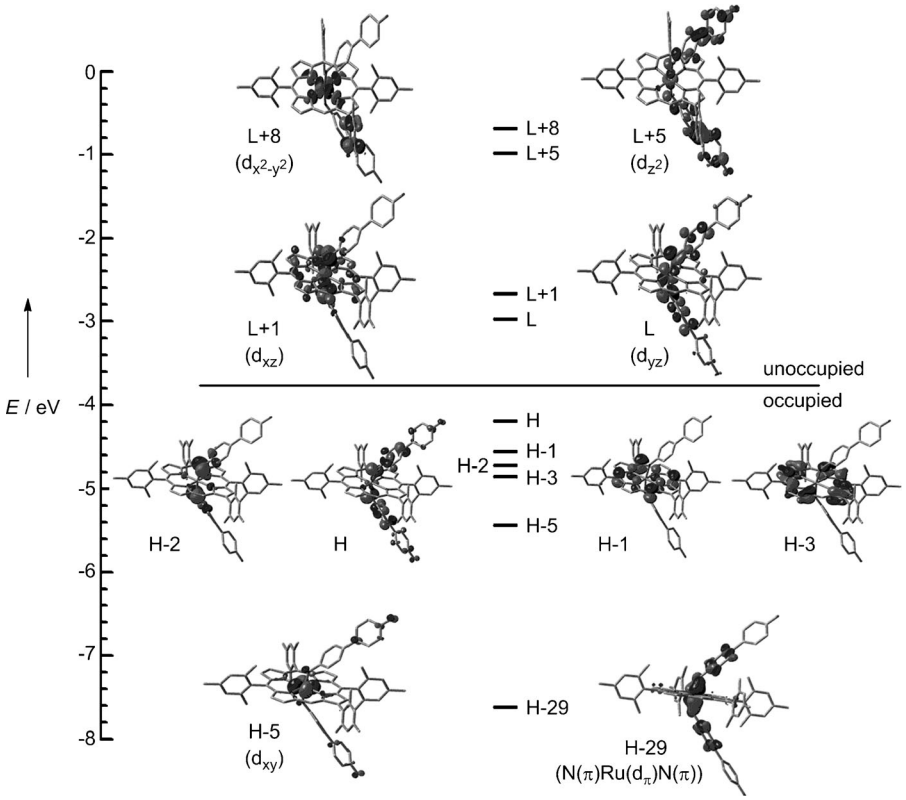


**Figure 9.** MO diagram of $[Ru^{VI}(tmp)(N\text{-}\mathbf{Ar}–\mathbf{Ar}\text{-}p\text{-}OH)_2]$ (isovalue = 0.04 a.u.). H = HOMO, L = LUMO.

slight mixing of the 2s and 2p orbitals of N(imide) atom leads to an appreciably bent $N_{imide}$-M-$N_{imide}$ (M = Ru, Os) axis that gives the *syn* configuration allowing for a better π-overlap between Ru/Os and N(imide) (Figure 10) and/or a better π-bonding along C–$N_{imide}$–M–$N_{imide}$–C (such as C21–N5–Ru1–N6–C33 in Figure 8).

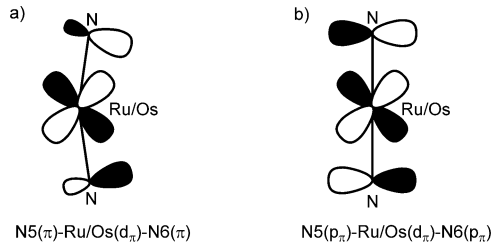


**Figure 10.** Schematic diagram showing: a) the N5–Ru/Os–N6 π-interaction with mixture of $p_\pi$ orbitals and s oribtals, b) the N5–Ru/Os–N6 π-interaction with pure $p_\pi$ orbitals.

### Reactivity of $[Ru^{IV}(por)(NHY)_2]$

**Reaction with bromine**: Treatment of $[Ru^{IV}(tmp)(NHY)_2]$ (Y = **Ar**–**Ar**, **Ar**^**Ar**, **Ar**–**Ar**–**Ar**) with a solution of bromine in dichloromethane caused the β band to be red-shifted from approximately 527 to about 541 nm within 7 min; meanwhile, the Soret band blue-shifted slightly from approximately 418 to about 416 nm, as revealed by UV/Vis measurements. After work up, the corresponding complexes $[Ru^{IV}(tmp)(NHY)Br]$ (**4**) were isolated in 51–69% yields, together with the N,N-coupling products Y–N=N–Y in 60–92% yields. The oxidative deprotonation products $[Ru^{VI}(tmp)(NY)_2]$ or $[Ru^{VI}(tmp)(NY)O]$ were not obtained from these reactions. Previously, bromine had been employed for the oxidation of $[Ru^{II}(por)(NH_2tBu)_2]$ to $[Ru^{VI}(por)(NtBu)O]$.[6d,22a] Related oxidation of $[Ru^{II}(por)(NH_3)_2]$ by *N*-bromosuccinimide was found to give $[Ru^{VI}(por)(N)Br]$.[41]

The $^1$H NMR spectra of the isolated $[Ru^{IV}(tmp)(NHY)Br]$ (Figure S3, for Y = **Ar**–**Ar**, in the Supporting Information) feature sharp signals at normal fields and show upfield-shifted $H_\beta$ signals ($\delta$ = 7.58–7.70 ppm) and downfield-shifted $H_o'$ and $H_m'$ signals compared with those of their $[Ru^{IV}(tmp)(NHY)_2]$ counterparts. For example, the $H_\beta/H_o'/H_m'$ signals are shifted from $\delta$ = 8.17/3.28/6.03 ppm for $[Ru^{IV}(tmp)(NH\{\mathbf{Ar}–\mathbf{Ar}\})_2]$ to $\delta$ = 7.69/4.20/6.10 ppm for $[Ru^{IV}(tmp)(NH\{\mathbf{Ar}–\mathbf{Ar}\})Br]$. In agreement with the unsymmetrical coordination at the axial sites in $[Ru^{IV}(tmp)(NHY)Br]$, the two *ortho*-methyl moieties of each *meso*-mesityl group in the tmp ligand give two well-separated signals.

**Reaction with PhI(OAc)$_2$**: We treated $[Ru^{IV}(por)(NHY)_2]$ (por = tmp, Y = **Ar**–**Ar**, **Ar**–**Ar**-*p*-OMe, **Ar**–**Ar**-*p*-Cl; por = ttp, Y = Ar-*p*-$NO_2$) with 4.5 equiv of $PhI(OAc)_2$ in $CDCl_3$ at 0 °C, and the reaction mixtures were monitored by $^1$H NMR spectroscopy. These reactions resulted in oxidative deprotonation to give $[Ru^{VI}(por)(NY)_2]$, which were subsequently converted to $[Ru^{VI}(por)(NY)O]$ and $[Ru^{VI}(por)O_2]$ possibly by hydrolysis in the presence of trace amounts of water in the solvent and/or imide-oxo exchange with PhI=O generated from $PhI(OAc)_2$ and water (Scheme 3). The three types of $Ru^{VI}$ complexes were identified on the basis of their $H_\beta$ chemical shifts (Table S8 in the Supporting Information). For a certain por ligand, replacement of the imide ligand(s) of $[Ru^{VI}(por)(NY)_2]$ by one and two oxo ligand(s) increases the $H_\beta$ chemical shift by 0.12–0.13 and 0.26–0.28 ppm, respectively (calculated from the data in Table S8 in the Supporting Information), similar to the corresponding increase of $H_\beta$ chemical shifts by 0.18 and 0.37 ppm, respectively, in the case of $[Ru^{VI}(ttp)(NtBu)_2]$ ($H_\beta$ 8.73),[6d] $[Ru^{VI}(ttp)(NtBu)O]$ ($H_\beta$ 8.91),[6d] and $[Ru^{VI}(ttp)O_2]$ ($H_\beta$ 9.1).[42]

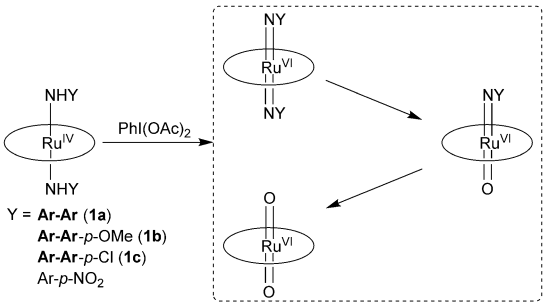


**Scheme 3.** Reactivity of $[Ru^{IV}(por)(NHY)_2]$ (**1**) with $PhI(OAc)_2$.

The $^1$H NMR spectra of the reaction mixture of $[Ru^{IV}(tmp)(NH\{\mathbf{Ar}–\mathbf{Ar}\text{-}p\text{-Cl}\})_2]$ with $PhI(OAc)_2$ at various reaction time of $t$ = 5–70 min are depicted in Figure S4 (in the Supporting Information) as examples. At $t$ = 5 min, two new $H_\beta$ signals with $\delta$ = 8.54 and 8.67 ppm appeared, which were assigned to $[Ru^{VI}(tmp)(N\{\mathbf{Ar}–\mathbf{Ar}\text{-}p\text{-Cl}\})_2]$ and $[Ru^{VI}(tmp)(N\{\mathbf{Ar}–\mathbf{Ar}\text{-}p\text{-Cl}\})O]$, respectively, with the former in larger amount. As the reaction time increased to $t$ = 15 min, the amount of the former substantially decreased whereas the amount of the latter increased accordingly (the starting complex was completely consumed), and another new $H_\beta$ signal with $\delta$ = 8.81 ppm assigned to $[Ru^{VI}(tmp)O_2]$[33] began to be discernible. Further increase of the reaction time to $t$ = 70 min led to disappearance of $[Ru^{VI}(tmp)(N\{\mathbf{Ar}–\mathbf{Ar}\text{-}p\text{-Cl}\})_2]$ and $[Ru^{VI}(tmp)(N\{\mathbf{Ar}–\mathbf{Ar}\text{-}p\text{-Cl}\})O]$, with $[Ru^{VI}(tmp)O_2]$ formed as the dominant complex in 87% yield (determined by $^1$H NMR spectroscopy).

The time required for the complete consumption of $[Ru^{IV}(tmp)(NHY)_2]$ increased along Y = **Ar**–**Ar**-*p*-Cl (15 min) < **Ar**–**Ar** (30 min) < **Ar**–**Ar**-*p*-OMe (40 min; Table S9 in the Supporting Information). This indicates that the electron-donating *para*-substituent on the arylamide ligand retards the reaction, in line with the increased basicity of the arylamide ligand which rendered it more difficult to be deprotonated.

### Nitrogen group transfer reactions with hydrocarbons

**Stoichiometric reactions of $[Ru^{VI}(tmp)(NY)_2]$**: The reactivity of bis(π-conjugated arylimide) complexes toward hydrocarbons was examined using $[Ru^{VI}(tmp)(NY)_2]$ (**3**, Y = **Ar**–**Ar**, **Ar**–**Ar**-*p*-Cl), together with cyclooctene and 1,2,3,4-tetrahydronaphthalene, and the results are depicted in Scheme 4 and Table 4. Reactions of the two arylimide complexes with cyclooctene in refluxing benzene for 6 h afforded the *N*-(π-conjugated aryl) aziridines **5a** and **5b** in 56–58% yields (determined by $^1$H NMR spectroscopy); similar reactions for 1,2,3,4-tetrahydronaphtha-

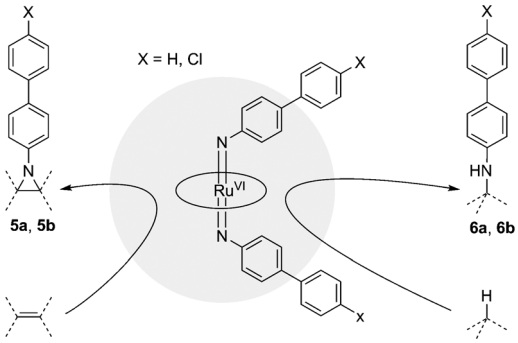


**Scheme 4.** Nitrogen group transfer/insertion reactions of $[Ru^{VI}(tmp)(NY)_2]$ (**3**).

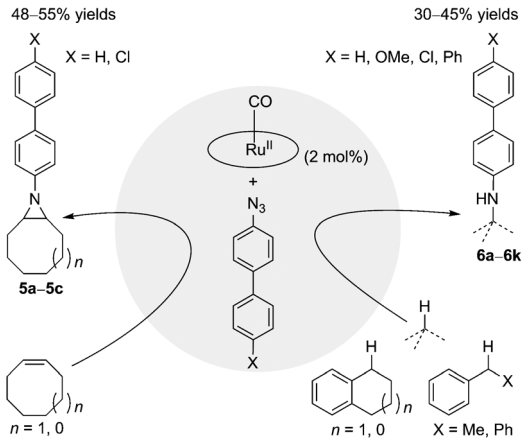


**Scheme 5.** Nitrogen group transfer/insertion reactions catalyzed by "$[Ru^{II}(tmp)(CO)] + N_3Y$".

lene gave benzylic C–H amination products **6a** and **6b** in 55–60% yields. Comparable yields of amination products were reported previously for the reactions of $[Ru^{VI}(tpp)(N\{Ar\text{-}3,5\text{-}CF_3\})_2]$ with hydrocarbons such as isobutyl benzene, which afforded the benzylic C–H amination product in 57% yield.[8a] Stoichiometric nitrogen group transfer/insertion reactions of $[Ru^{VI}(por)(NSO_2\{Ar\text{-}p\text{-}X\})_2]$ (X = OMe, Me, H, Cl, $NO_2$) with various alkenes and alkanes have also been reported, with yields of up to 88% being obtained for the resulting *N*-sulfonyl aziridines/amines.[15]

**Catalytic reactions with "$[Ru^{II}(tmp)(CO)] + N_3Y$"**: We then examined the catalytic nitrogen group transfer/insertion reactions using $[Ru^{II}(tmp)(CO)]$ as the catalyst, in view of its reaction with the π-conjugated aryl azides $N_3Y$ (Y = **Ar**–**Ar**, **Ar**–**Ar**-*p*-OMe, **Ar**–**Ar**-*p*-Cl, **Ar**–**Ar**–**Ar**) to give $[Ru^{VI}(tmp)(NY)_2]$ (**3**). Treatment of cyclooctene and cycloheptene in refluxing benzene with $N_3Y$ (Y = **Ar**–**Ar**, **Ar**–**Ar**-*p*-Cl) in the presence of $[Ru^{II}(tmp)(CO)]$ (2 mol%) for 13–15 h gave the corresponding aziridines **5a**–**5c** in 48–55% isolated yields (Scheme 5; entries 1–3, Table S10 in the Supporting Information). For benzylic hydrocarbons including 1,2,3,4-tetrahydronaphthalene, indan, diphenylmethane, and ethylbenzene, their reactions with $N_3Y$ (Y = **Ar**–**Ar**, **Ar**–**Ar**-*p*-OMe, **Ar**–**Ar**-*p*-Cl, **Ar**–**Ar**–**Ar**) catalyzed by $[Ru^{II}(tmp)(CO)]$ (2 mol%) under similar conditions for 24–30 h afforded benzylic C–H amination products **6a**–**6k** in 30–45% yields (Scheme 5; entries 4–14, Table S10 in the Supporting Information).

The moderate product yields using "$[Ru^{II}(tmp)(CO)] + N_3Y$" protocol could partially be attributed to the sterically encumbered porphyrin ligand in catalyst $[Ru^{II}(tmp)(CO)]$ rendering the ruthenium–arylimide/nitrene intermediate to be less reactive. $[Ru^{IV}(por)Cl_2]$ were previously reported to be effective catalysts for C–H bond oxidation and alkene epoxidation with 2,6-$Cl_2$pyNO,[43] and aldehyde C–H amination with phosphoryl azides.[44] Upon changing the catalyst from $[Ru^{II}(tmp)(CO)]$ to $[Ru^{IV}(ttp)Cl_2]$, the yield of the *N*-(π-conjugated aryl) aziridine **5a** increased from 50 to 65% for the aziridination of cyclooctene with $N_3$(**Ar**–**Ar**), and the yields of *N*-(π-conjugated aryl) amines **6c** and **6j** increased from 40 to 51% and 55% for the benzylic C–H amination of 1,2,3,4-tetrahydronaphthalene and ethylbenzene, respectively, with $N_3$(**Ar**–**Ar**-*p*-OMe). Diazene compounds, which probably came from coupling reaction of the ruthenium arylimide/nitrene intermediates, were the major byproducts in these nitrogen group transfer/insertion reactions.

**Table 4.** Stoichiometric reaction of $[Ru^{VI}(tmp)(NY)_2]$ (**3**) with hydrocarbons.[a]

| Y | Hydrocarbon | Product | Yield [%][b] |
|---|---|---|---|
| **Ar**–**Ar** (**3a**) |  | 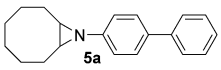 **5a** | 56 |
| **Ar**–**Ar**-*p*-Cl (**3c**) |  | 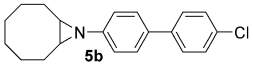 **5b** | 58 |
| **Ar**–**Ar** (**3a**) |  | 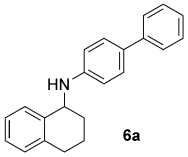 **6a** | 60 |
| **Ar**–**Ar**-*p*-Cl (**3c**) |  | 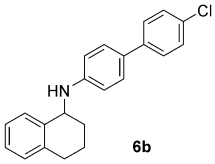 **6b** | 55 |

[a] Reaction conditions: $[Ru^{VI}(tmp)(NY)_2]$ (0.1 mmol), hydrocarbons (2 mL), benzene (1 mL), refluxing under $N_2$, 6 h. [b] $^1$H NMR yield using 1,1-diphenylethylene as the internal standard.

## General remarks

The development of reactive high-valent ruthenium–imide complexes supported by porphyrin ligands is instrumental in elucidating the mechanisms and expanding the scope of ruthenium porphyrin-mediated nitrogen group transfer/insertion reactions. To date, the following types of ruthenium–imide porphyrin complexes have been isolated: 1) $Ru^{VI}$–oxo(alkyli-

mide) complexes [$Ru^{VI}$(por)(N*t*Bu)O], together with their osmium analogues [$Os^{VI}$(por)(N*t*Bu)O] and [$Os^{VI}$(por)(N*t*Bu)$_2$], prepared in our group in 1992[22a] from oxidative deprotonation of [$M^{II}$(por)($NH_2$*t*Bu)$_2$] (M = Ru or Os) with bromine or air; 2) $Ru^{IV}$–mono(arylimide) complexes [$Ru^{IV}$(por)(N{Ar-*p*-X})] prepared by Leung and co-workers[11] in 1997 from reaction of [$Ru^{IV}$(por)$Cl_2$] with $NH_2$(Ar-*p*-X); 3) $Ru^{VI}$–bis(sulfonylimide) complexes [$Ru^{VI}$(por)($NSO_2${Ar-*p*-X})$_2$] synthesized by Che and co-workers in 1999[15b] and 2005[15d] by treatment of [$Ru^{II}$(por)(CO)] with PhI=$NSO_2$(Ar-*p*-X); 4) $Ru^{VI}$–bis(arylimide) complexes [$Ru^{VI}$(tpp)(N{Ar-*p*-$NO_2$})$_2$] prepared by Smieja and co-workers in 2002 from the reaction of [$Ru^{II}$(ttp)]$_2$ with $N_3$(Ar-*p*-$NO_2$),[13b] and [$Ru^{VI}$(tpp)(N{Ar-3,5-$CF_3$})$_2$] prepared by Cenini, Gallo, and co-workers in 2009 from the reaction of [$Ru^{II}$(por)(CO)] with $N_3$(Ar-3,5-$CF_3$).[8a] Of these ruthenium–imide porphyrin complexes, [$Ru^{VI}$(tpp)(N{Ar-3,5-$CF_3$})$_2$][8a] and [$Ru^{VI}$(tmp)($NSO_2${Ar-*p*-OMe})$_2$][36] have been structurally characterized by X-ray crystal analysis.

Nitrogen group transfer/insertion reactions of isolated ruthenium–imide porphyrin complexes are hitherto focused on alkene aziridination and C–H amination by [$Ru^{VI}$(por)($NSO_2${Ar-*p*-X})$_2$],[15] together with C–H amination by [$Ru^{VI}$(tpp)(N{Ar-3,5-$CF_3$})$_2$].[8a] The osmium(VI) analogues [$Os^{VI}$(por)$(NY)_2$][13] and [$Os^{VI}$(por)($NSO_2$Y)$_2$][45] have not been found to exhibit such reactivities. In general, metal–imides that are reactive toward alkene aziridination and/or C–H amination remain sparse.[8,14,15]

One of the well-documented approaches to metal–imide/nitrene complexes is the use of aryl azides as the imide/nitrene source.[8,9,13] Organic azides are an attractive source of imide/nitrene owing to the nonhazardous nature of the byproduct $N_2$. There are various types of organic azides known in the literature. Besides aryl azides, typical organic azides employed as nitrene source in catalysis include sulfonyl azides, alkoxycarbonyl azides, and phosphoryl azides.[46] On the basis of previous synthesis of [$Cr^{IV}$(por)(NY)][9] and [$M^{VI}$(por)$(NY)_2$] (M = Ru, Os)[8,13] from aryl azides, organic azides would be useful imide/nitrene source for preparation of metal–imide/nitrene porphyrin complexes.

Incorporation of π-conjugated aryl groups into the imide ligands has the potential to generate metal–imides that feature extensive delocalization involving metal–nitrogen multiple bonds and/or allow the study of electronic communication between redox active high-valent metal ions and remote functional groups, as well as undergo nitrogen group transfer/insertion reactions to produce aziridines/amines bearing π-conjugated aryl groups. The present work has expanded the reactive metal–imide complexes to the π-conjugated arylimides and has demonstrated the formation of *N*-(π-conjugated aryl) aziridines/amines by nitrogen-group transfer/insertion reactions of well-defined metal–imide complexes. [$Ru^{IV}$(tmp)$(NHY)_2$] (Y = **Ar**–**Ar**-*p*-OMe, **Ar**–**Ar**-*p*-Cl, and **Ar**^**Ar**) and [$Ru^{VI}$(tmp)(N{**Ar**–**Ar**-*p*-OMe})$_2$] are unique examples of structurally characterized *trans*-metal–bis(π-conjugated arylamide) and *trans*-metal–bis(π-conjugated arylimide) complexes, respectively; the latter also contributes a structurally characterized metalloporphyrin with π-conjugated arylimide ligand(s).

## Conclusion

[$Ru^{IV}$(por)$(NHY)_2$] and [$Ru^{VI}$(por)$(NY)_2$] complexes bearing π-conjugated arylamide and π-conjugated arylimide ligands, respectively, have been prepared and characterized by spectroscopic means and X-ray crystal structure determinations. A combination of π-conjugated arylimide and sterically encumbered porphyrin ligands allows the preparation of ruthenium–bis(arylimide) complexes without the need to introduce a strongly electron-withdrawing group onto the arylimide ligand. The extent of π-conjugation in the arylamide and arylimide ligands slightly affects the spectral properties of the complexes and the Ru–N(arylamide/arylimide) distances. Electrochemical studies on [$Ru^{IV}$(por)$(NHY)_2$] revealed considerable effect of the π-conjugated arylamide ligands on the metal-centered reduction and oxidation potentials. DFT calculations on [$Ru^{VI}$(tmp)(N{**Ar**–**Ar**-*p*-OH})$_2$] lend support for the $d^2$ $Ru^{VI}$ formulation of [$Ru^{VI}$(por)$(NY)_2$] and provide insight into their *syn* configuration revealed by X-ray crystal structure determination.

The [$Ru^{IV}$(por)$(NHY)_2$] and [$Ru^{VI}$(por)$(NY)_2$] complexes undergo interesting redox and/or C–N bond formation reactions. [$Ru^{IV}$(por)(NHY)Br] are formed in the reaction of [$Ru^{IV}$(por)$(NHY)_2$] with bromine. Oxidation of [$Ru^{IV}$(por)$(NHY)_2$] using PhI$(OAc)_2$ affords [$Ru^{VI}$(por)$(NY)_2$], which demonstrates the generation of metal–imide complexes by oxidative deprotonation with a PhI$(OR)_2$ oxidant. [$Ru^{VI}$(tmp)$(NY)_2$] undergo stoichiometric alkene aziridination and C–H amination reactions to give *N*-(π-conjugated aryl) aziridines and amines, respectively, in moderate yields. The corresponding catalytic nitrogen group transfer/insertion reactions with comparable product yields can be achieved using a "[$Ru^{II}$(tmp)(CO)] + π-conjugated aryl azide" protocol.

## Acknowledgements

We gratefully acknowledge The University of Hong Kong, the Hong Kong Research Grants Council (HKU, 700813), and the National Natural Science Foundation of China (NSFC, 21272197) for financial support.

**Keywords:** metal–amide complexes · metal–imide complexes · N ligands · porphyrinoids · ruthenium

[1] F. A. Cotton, G. Wilkinson, C. Murillo, M. Bochmann, *Advanced Inorganic Chemistry*, 6th ed, Wiley, New York, **1999**.

[2] W. A. Nugent, J. M. Mayer, *Metal–Ligand Multiple Bonds*, Wiley, New York, **1988**.

[3] Abbreviations of the porphyrin ligands involved in this study: oep = 2,3,7,8,12,13,17,18-octaethylporphyrinato(2−); $por^0$ = the simplest porphyrinato(2−) ligand; tbpp = 5,10,15,20-tetrakis(*p*-*tert*-butylphenyl)porphyrinato(2−); tmp = 5,10,15,20-tetramesitylporphyrinato(2−); tpp = 5,10,15,20-tetraphenylporphyrinato(2−); 4-Cl-tpp = 5,10,15,20-tetrakis(4-chlorophenyl)porphyrinato(2−); 3,5-Cl-tpp = 5,10,15,20-tetrakis(3,5-dichlorophenyl)porphyrinato(2−); $F_{20}$-tpp = 5,10,15,20-tetrakis(pentafluorophenyl)porphyrinato(2−); 4-OMe-tpp = 5,10,15,20-tetrakis(4-methoxyphenyl)porphyrinato(2−); 3,4,5-OMe-tpp = 5,10,15,20-tetrakis(3,4,5-trimethoxyphenyl)porphyrinato(2−); ttp = 5,10,15,20-tetrakis(4-methylphenyl)porphyrinato(2−).

[4] For examples, see: a) C. J. Jones, J. A. McCleverty, B. D. Neaves, S. J. Reynolds, H. Adams, N. A. Bailey, G. Denti, *J. Chem. Soc. Dalton Trans.* **1986**, 733; b) J. D. Masuda, K. C. Jantunen, B. L. Scott, J. L. Kiplinger, *Organometallics* **2008**, *27*, 803.

[5] For examples, see: a) J. Chatt, J. D. Garforth, N. P. Johnson, G. A. Rowe, *J. Chem. Soc.* **1964**, 1012; b) J. W. Buchler, S. Pfeifer, *Z. Naturforsch. B* **1985**, *40*, 1362; c) G. R. Clark, A. J. Nielson, C. E. F. Rickard, *J. Chem. Soc. Dalton Trans.* **1996**, 4265; d) G. Hogarth, T. Norman, S. P. Redmond, *Polyhedron* **1999**, *18*, 1221; e) G. Hogarth, D. G. Humphrey, N. Kaltsoyannis, W.-S. Kim, M.-y. Lee, T. Norman, S. P. Redmond, *J. Chem. Soc. Dalton Trans.* **1999**, 2705.

[6] a) C.-M. Che, J.-S. Huang, Z.-Y. Li, C.-K. Poon, *Inorg. Chim. Acta* **1991**, *190*, 161; b) J.-S. Huang, C.-M. Che, Z.-Y. Li, C.-K. Poon, *Inorg. Chem.* **1992**, *31*, 1313; c) Z.-Y. Li, J.-S. Huang, M. C.-W. Chan, K.-K. Cheung, C.-M. Che, *Inorg. Chem.* **1997**, *36*, 3064; d) J.-S. Huang, X.-R. Sun, S. K.-Y. Leung, K.-K. Cheung, C.-M. Che, *Chem. Eur. J.* **2000**, *6*, 334; e) S. K.-Y. Leung, J.-S. Huang, N. Zhu, C.-M. Che, *Inorg. Chem.* **2003**, *42*, 7266.

[7] a) S. D. Gray, J. L. Thorman, L. M. Berreau, L. K. Woo, *Inorg. Chem.* **1997**, *36*, 278; b) J. L. Thorman, I. A. Guzei, V. G. Young, Jr., L. K. Woo, *Inorg. Chem.* **1999**, *38*, 3814; c) J. L. Thorman, I. A. Guzei, V. G. Young, Jr., L. K. Woo, *Inorg. Chem.* **2000**, *39*, 2344.

[8] a) S. Fantauzzi, E. Gallo, A. Caselli, F. Ragaini, N. Casati, P. Macchi, S. Cenini, *Chem. Commun.* **2009**, 3952; b) D. Intrieri, A. Caselli, F. Ragaini, P. Macchi, N. Casati, E. Gallo, *Eur. J. Inorg. Chem.* **2012**, 569.

[9] a) R. L. Elliott, P. J. Nichols, B. O. West, *Polyhedron* **1987**, *6*, 2191; b) B. Moubaraki, K. S. Murray, P. J. Nichols, S. Thomson, B. O. West, *Polyhedron* **1994**, *13*, 485.

[10] a) L. M. Berreau, V. G. Young, Jr., L. K. Woo, *Inorg. Chem.* **1995**, *34*, 527; b) S. D. Gray, J. L. Thorman, V. Adamian, K. M. Kadish, L. K. Woo, *Inorg. Chem.* **1998**, *37*, 1; c) L. M. Berreau, J. Chen, L. K. Woo, *Inorg. Chem.* **2005**, *44*, 7304.

[11] W.-H. Leung, T. S. M. Hun, H.-w. Hou, K.-Y. Wong, *J. Chem. Soc. Dalton Trans.* **1997**, 237.

[12] C.-X. Yin, J. M. Stryker, M. R. Gray, *Energy Fuels* **2009**, *23*, 2600.

[13] a) J. A. Smieja, K. M. Omberg, G. L. Breneman, *Inorg. Chem.* **1994**, *33*, 614; b) J. A. Smieja, K. Shirzad, M. Roy, K. Kittilstved, B. Twamley, *Inorg. Chim. Acta* **2002**, *335*, 141.

[14] a) R. Waterman, G. L. Hillhouse, *J. Am. Chem. Soc.* **2003**, *125*, 13350; b) C. A. Laskowski, A. J. M. Miller, G. L. Hillhouse, T. R. Cundari, *J. Am. Chem. Soc.* **2011**, *133*, 771; c) E. R. King, E. T. Hennessy, T. A. Betley, *J. Am. Chem. Soc.* **2011**, *133*, 4917.

[15] a) S.-M. Au, W.-H. Fung, M.-C. Cheng, C.-M. Che, S.-M. Peng, *Chem. Commun.* **1997**, 1655; b) S.-M. Au, J.-S. Huang, W.-Y. Yu, W.-H. Fung, C.-M. Che, *J. Am. Chem. Soc.* **1999**, *121*, 9120; c) J.-L. Liang, J.-S. Huang, X.-Q. Yu, N. Zhu, C.-M. Che, *Chem. Eur. J.* **2002**, *8*, 1563; d) S. K.-Y. Leung, W.-M. Tsui, J.-S. Huang, C.-M. Che, J.-L. Liang, N. Zhu, *J. Am. Chem. Soc.* **2005**, *127*, 16629.

[16] Selected examples for biphenyl-4-yl nitrenes: a) R. A. McClelland, P. A. Davidse, G. Hadzialic, *J. Am. Chem. Soc.* **1995**, *117*, 4173; b) R. A. McClelland, M. J. Kahley, P. A. Davidse, G. Hadzialic, *J. Am. Chem. Soc.* **1996**, *118*, 4794; c) T. Harder, P. Wessig, J. Bendig, R. Stösser, *J. Am. Chem. Soc.* **1999**, *121*, 6580; d) M.-L. Tsao, N. Gritsan, T. R. James, M. S. Platz, D. A. Hrovat, W. T. Borden, *J. Am. Chem. Soc.* **2003**, *125*, 9343; e) G. Burdzinski, J. C. Hackett, J. Wang, T. L. Gustafson, C. M. Hadad, M. S. Platz, *J. Am. Chem. Soc.* **2006**, *128*, 13402; f) J. Wang, G. Burdzinski, Z. Zhu, M. S. Platz, C. Carra, T. Bally, *J. Am. Chem. Soc.* **2007**, *129*, 8380.

[17] Selected examples for 4-(phenylethynyl)phenyl nitrenes: a) S. Murata, H. Iwamura, *J. Am. Chem. Soc.* **1991**, *113*, 5547; b) H. Tomioka, S. Sawai, *Org. Biomol. Chem.* **2003**, *1*, 4441.

[18] A. Sasaki, L. Mahé, A. Izuoka, T. Sugawara, *Bull. Chem. Soc. Jpn.* **1998**, *71*, 1259.

[19] For dirhodium- and iron-catalyzed intramolecular C–N bond forming reactions of aryl azides including a few biphenyl-4-yl azides, see: a) Q. Nguyen, K. Sun, T. G. Driver, *J. Am. Chem. Soc.* **2012**, *134*, 7262; b) Q. Nguyen, T. Nguyen, T. G. Driver, *J. Am. Chem. Soc.* **2013**, *135*, 620.

[20] For dirhodium-catalyzed intermolecular C–H amination of benzamides with aryl azides including the amination of a benzamide with $N_3$(**Ar**–**Ar**), see: J. Ryu, K. Shin, S. H. Park, J. Y. Kim, S. Chang, *Angew. Chem.* **2012**, *124*, 10042; *Angew. Chem. Int. Ed.* **2012**, *51*, 9904.

[21] For dirhodium- and ruthenium-catalyzed intramolecular C–N-bond forming reactions of aryl azides including biphenyl-2-yl azides, see: a) B. J. Stokes, B. Jovanović, H. Dong, K. J. Richert, R. D. Riell, T. G. Driver, *J. Org. Chem.* **2009**, *74*, 3225; b) W. G. Shou, J. Li, T. Guo, Z. Lin, G. Jia, *Organometallics* **2009**, *28*, 6847.

[22] a) J.-S. Huang, C.-M. Che, C.-K. Poon, *J. Chem. Soc. Chem. Commun.* **1992**, 161; b) J.-S. Huang, S. K.-Y. Leung, K.-K. Cheung, C.-M. Che, *Chem. Eur. J.* **2000**, *6*, 2971.

[23] A. J. Bailey, B. R. James, *Chem. Commun.* **1996**, 2343.

[24] C. Morice, P. Le Maux, C. Moinet, G. Simonneaux, *Inorg. Chim. Acta* **1998**, *273*, 142.

[25] J.-S. Huang, S. K.-Y. Leung, Z.-Y. Zhou, N. Zhu, C.-M. Che, *Inorg. Chem.* **2005**, *44*, 3780.

[26] X.-R. Sun, J.-S. Huang, K.-K. Cheung, C.-M. Che, *Inorg. Chem.* **2000**, *39*, 820.

[27] D. C. Barman, P. Saikia, D. Prajapati, J. S. Sandhu, *Synth. Commun.* **2002**, *32*, 3407.

[28] A. Shaabani, D. G. Lee, *Tetrahedron Lett.* **2001**, *42*, 5833.

[29] K. Orito, T. Hatakeyama, M. Takeo, S. Uchiito, M. Tokuda, H. Suginome, *Tetrahedron* **1998**, *54*, 8403.

[30] F. Benedini, M. Nali, B. Rindone, S. Tollari, S. Cenini, G. La Monica, F. Porta, *J. Mol. Catal.* **1986**, *34*, 155.

[31] Further purification of the $[Ru^{VI}(por)(NY)_2]$ complexes by flash chromatography proved difficult, as they were found to be not stable on silica gel or alumina.

[32] It has been documented that the $H_\beta$ chemical shifts of diamagnetic metalloporphyrins usually increase with the oxidation state of the metal ion. See: a) A. Antipas, J. W. Buchler, M. Gouterman, P. D. Smith, *J. Am. Chem. Soc.* **1980**, *102*, 198; b) H. Scheer, J. J. Katz, in *Porphyrins and Metalloporphyrins* (Ed.: K. M. Smith), Elservier, Amsterdam, **1975**, p. 399.

[33] J. T. Groves, R. Quinn, *Inorg. Chem.* **1984**, *23*, 3844.

[34] The isomers are stable in both solid state and dichloromethane solution; no conversion of one isomer to another was observed in solution after a week at room temperature, as revealed by $^1$H NMR spectroscopy measurements. Attempts to separate the isomers by recrystallization and column chromatography have not been successful.

[35] CCDC-638450 ($[Ru^{IV}(tmp)(NHY)_2]$ (Y = **Ar**–**Ar**-*p*-Cl)), -638451 ($[Ru^{IV}(tmp)(NHY)_2]$ (Y = **Ar**–**Ar**–*p*-OMe)), -638452 ($[Ru^{IV}(tmp)(NHY)_2]$ (Y = **Ar**^**Ar**)) and -795707 ($[Ru^{VI}(tmp)(N\{$**Ar**–**Ar**-*p*-OMe$\})_2]$) contain the supplementary crystallographic data for this paper. These data can be obtained free of charge from The Cambridge Crystallographic Data Centre via www.ccdc.cam.ac.uk/data_request/cif.

[36] Z. Guo, X. Guan, J.-S. Huang, W.-M. Tsui, Z. Lin, C.-M. Che, *Chem. Eur. J.* **2013**, *19*, 11320.

[37] C.-Y. Chen, S.-H. Cheng, Y. O. Su, *J. Electroanal. Chem.* **2000**, *487*, 51.

[38] W.-M. Tsui, Ph.D. thesis, The University of Hong Kong, **2006**.

[39] Y. Li, J.-S. Huang, G.-B. Xu, N. Zhu, Z.-Y. Zhou, C.-M. Che, K.-Y. Wong, *Chem. Eur. J.* **2004**, *10*, 3486.

[40] E. Gonzalez, P. J. Brothers, A. Ghosh, *J. Phys. Chem. B* **2010**, *114*, 15380.

[41] S. K.-Y. Leung, J.-S. Huang, J.-L. Liang, C.-M. Che, Z.-Y. Zhou, *Angew. Chem.* **2003**, *115*, 354; *Angew. Chem. Int. Ed.* **2003**, *42*, 340.

[42] C. Ho, W.-H. Leung, C.-M. Che, *J. Chem. Soc. Dalton Trans.* **1991**, 2933.

[43] J.-L. Zhang, C.-M. Che, *Chem. Eur. J.* **2005**, *11*, 3899.

[44] W. Xiao, C.-Y. Zhou, C.-M. Che, *Chem. Commun.* **2012**, *48*, 5871.

[45] a) S.-M. Au, W.-H. Fung, J.-S. Huang, K.-K. Cheung, C.-M. Che, *Inorg. Chem.* **1998**, *37*, 6564; b) Y. Li, J.-S. Huang, Z.-Y. Zhou, C.-M. Che, *J. Am. Chem. Soc.* **2001**, *123*, 4843.

[46] For reviews, see: a) S. Cenini, E. Gallo, A. Caselli, F. Ragaini, S. Fantauzzi, C. Piangiolino, *Coord. Chem. Rev.* **2006**, *250*, 1234; b) T. G. Driver, *Org. Biomol. Chem.* **2010**, *8*, 3831; c) B. J. Stokes, T. G. Driver, *Eur. J. Org. Chem.* **2011**, 4071; d) S. Cenini, F. Ragaini, E. Gallo, A. Caselli, *Curr. Org. Chem.* **2011**, *15*, 1578.

Received: December 31, 2013
Revised: May 30, 2014
Published online on July 25, 2014